ESTIMATION OF THE BREAKAGE FUNCTION OF A ROLLER MILL CRUSHING QUARTZITE

by

GRACE MULOLWA TSHINGUZ

Submitted in accordance with the requirements for the degree of

MASTER OF TECHNOLOGY

in the

DEPARTMENT OF CHEMICAL ENGINEERING

at the

UNIVERSITY OF SOUTH AFRICA

Supervisors: Prof. Diane Hildebrandt

Dr Clayton Bhondayi

2020

DECLARATION

Full names and surname: Grace Mulolwa Tshinguz

Student number: 61972053

Degree: Master of Technology

TOPIC: ESTIMATION OF THE BREAKAGE FUNCTION OF A ROLLER MILL CRUSHING QUARTZITE

I declare that the above dissertation is my own work and that all the sources that I have used or quoted have been indicated and acknowledged by means of complete references.

I further declare that I submitted the dissertation to originality checking software and that it falls within the accepted requirements for originality.

I further declare that I have not previously submitted this work, or part of it, for examination at Unisa for another qualification, or to any other higher education institution.

Signature:

Date:

ABSTRACT

Studies on the breakage function of roller mills are limited. The approach of using breakage functions adapted from other milling systems has been previously used to model the breakage of laboratory roller mills.

However, in most cases this approach has been found to be inadequate because the assumption of normalization used for modelling other milling systems may not apply to roller mills.

This study assumes the non-normalization of the model for roller milling. It aims to define the breakage function of roller milling of quartzite and to develop a predictive model for first breakage for a laboratory roller mill.

Six size fractions of quartzite were prepared using a Jaw Crusher for primary breakage of a quartzite feed material. The product from the crusher was split into narrow size ranges using a sieve shaker. Each size fraction was in turn split into three samples, which were then fed separately to the roller mill, using a different roll gap for each sample. A breakage matrix for each roll gap size was then generated from the product size analysis of the sample. Using the cumulative passing and the milling ratio, the analysis of the three breakage matrices led to the definition of the breakage function. The coefficients of the breakage function were curve-fitted, in order to develop a predictive model.

The results indicate that the assumption of non-normalization is appropriate for roller milling of quartzite rock. The breakage function follows a log-normal trend for all the feed size fractions used, and the coefficients of the breakage function can be fitted by polynomial functions of second degree of the feed size. Further research is needed to investigate the correlation of the breakage function and the product size.

Key words: roller mill; quartzite; breakage matrix; breakage function; assumption of non-normalization; milling-ratio.

DEDICATION

This study is dedicated to: my parents, Celestin Matuka Tshinguz and Victorine Kakazi wa Mulolwa; and my family for their love and support.

ACKNOWLEDGEMENT

First and foremost, praises and thanks to God, the Almighty, for the gift of the Holy Spirit.

I would like to express my deep and sincere gratitude to my research supervisors, Professor Diane Hildebrandt and Doctor Clayton Bhondayi, for giving me the opportunity to do research and for providing invaluable guidance throughout this research. Their dynamism, vision, sincerity and motivation inspired me deeply. They taught me the methodology that was used to carry out the research and present the research work as clearly as possible. It was a great privilege and honor to work and study under their guidance.

The completion of this project could not have been accomplished without the support of the comminution team of IDEAS group.

I extend my gratitude to someone special in my life, the future mother of my kids, for her support and assistance.

I cannot forget my family in Christ Jesus, for their spiritual support.

I would also like to acknowledge UNISA and NRF for the financial support provided.

TABLE OF CONTENTS

LIST OF TABLES

LIST OF FIGURES

Chapter 1. Introduction

1.1 Background

The earth's crust is composed of rocks and rocks, in turn, are composed of valuable and non-valuable minerals. Minerals play an essential role in the development of civilizations and the industrial economy. The study or process of liberating valuable minerals from the non-valuable minerals, using size reduction, is called "comminution".

Comminution aims to optimize the production of material of a specified size of interest. This could be the liberation size or the required size for aggregates, for example. Therefore, many studies have been performed using different types of comminution equipment, in order to find relationships between the size distribution of the material in the product and feed, the operating conditions of the equipment and the properties of the material (Campbell and Webb, 2001).

The mathematical equation that relates the size distribution of the material of the product to the size distribution of the feed is called the breakage equation (Campbell and Webb, 2001). The discretization of the breakage equation results in a matrix called the breakage matrix (Broadbent and Callcott, 1956), which in turn leads to the definition of the breakage function. The breakage function describes the size distribution of a material in the product obtained from the breakage of a feed of a single or mono particle size.

There are two very different, and indeed contradictory, assumptions used to model the breakage function. The breakage function is assumed to be either normalizable or, conversely, non-normalizable. Normalization assumes that the size distribution of the material in the product does not depend on the feed's size distribution. In contrast, the non-normalization assumption considers the impact of the size distribution of the feed on the size distribution of the product.

1.2 Problem statement

The normalization assumption is used to reduce the number of parameters that describe the breakage function (Austin et.al., 1984). However, it is recognized that the assumption is often invalid for ball milling (Austin and Bhatia, 1971), or even milling studies in general (Reid, 1965). A modification to the normalized breakage function was introduced by Austin and Luckie (1972) to account for non-normalized breakage to improve the accuracy of the breakage model.

Roller milling is an important size reduction operation in the production of minerals and ores, of specific sizes. Haque (1991) states that the breakage equation for roller milling is different from that of other milling systems. Therefore, a specific breakage function for roller milling should be defined.

Campbell and Webb (2001) used a roller mill to break wheat. They used a non-normalized breakage function to define the breakage of wheat in the roller mill. They showed that the breakage function depended on the ratio of the roll gap to the input particle size, which they called the milling ratio. They also showed that the breakage function for wheat was linear with respect to product particle size for a constant milling ratio.

This research aimed to determine the breakage function of a laboratory roller mill, using quartzite rocks as the feed. Modelling the breakage of quartzite in a roller mill is interesting, because the breakage function for roller milling of quartzite has not been determined previously. This research also investigated if the breakage of quartzite in a roller mill is normalizable or non-normalizable, and whether or not the approach used by Campbell and Webb to model the breakage function for wheat can be applied to quartzite.

1.3 Research questions

The following research questions were considered:

1) What breakage function describes the product particle size distribution for roller milling of feeds of quartzite of different narrow (mono) sizes?

2) Is the breakage function non-normalizable or normalizable?
3) Can elements of the breakage function be correlated to mill operating parameters, such as the milling ratio, using Campbell and Webb's approach?

1.4 Objectives

The following objectives were defined:

1) Construct the breakage matrices for different gap sizes of the roller mill and various mono size feeds. The breakage function can then be analyzed to determine if it is normalizable or non-normalizable.
2) Use the cumulative passing distribution and the milling ratio to analyse the breakage function and determine the parameters that describe the breakage function.
3) Use the approach applied by Campbell and Webb to determine if the parameters of the breakage function can be correlated with the milling ratio.

1.5 Delimitation

The variables used for modeling in this project are limited by the particle size distribution for the material and the gap size for the roller mill.

1.6 Layout of the dissertation

The dissertation is divided into five chapters, namely:

Chapter 1: It describes the background and the problem statement of this dissertation. It also formulates the research questions, objectives and the delimitations of the project.

Chapter 2: It introduces the theory of comminution and reviews the literature on breakage in general, and on roller mills in particular. The methods and approaches used by other researchers, in modelling roller mills are discussed, including that used by Campbell and Webb(2001).

Chapter 3: It describes the materials used for breakage, the experimental equipment, and the methods used for this research.

Chapter 4: It presents the experimental results, which are then used to determine the roller mill's breakage function. The breakage function is analyzed using the approach used by Campbell and Webb (2001), and the dependence of this function on the roll gap is determined.

Chapter 5: This chapter presents the conclusion and the recommendations of this study

Chapter 2: Literature Review

This chapter comprises three sections.

The first section reviews quartzite, which is used for the experimental work in this project. This section is, in turn, divided into two sub-sections. The first sub-section presents an overview of minerals in general, and describes the main mineral in quartzite, namely quartz. The second sub-section focuses on the properties of quartzite and discusses some of its uses. The second section introduces the methods used to extract minerals from the ground. This section also presents the objectives of comminution and a brief description of a roller mill as a secondary crusher. The third section introduces the modeling of comminution systems, and comprises three sub-sections:

- The first sub-section introduces the breakage equation. The breakage equation relates the feed and product size distributions and can be established using the probability density function.
- The breakage matrix is introduced next. The discretization of the breakage equation leads to the concept of a breakage matrix. For illustration purposes, some previous work, particularly work done on roller milling, is described.
- Finally, the breakage function is discussed. It relates the product size distribution of the product to a mono or narrow sized feed. Previous research on correlating the elements of breakage function to the operating parameters of a roller mill, such as gap size, are reviewed.

2.1 Overview of quartzite rock and its properties

2.1.1 Origin and definition

The earth's crust is composed of rocks, and these rocks are, in turn, associations of minerals (Wilson, 2010). The term mineral describes a solid substance that occurs naturally in the earth's crust and which has a specific chemical composition and crystal structure (Aydinap, 2012). Among

the 12 major common chemical elements found in the earth's crust (oxygen, silicon, aluminum, iron, calcium, sodium, potassium, magnesium, titanium, hydrogen, manganese and phosphorus), silicon and oxygen comprise more than 70 percent of the total, by weight (Rudnick & Foutain, 1995). Therefore silicates, also called silicon dioxide (SiO_2), are the most abundant mineral in the earth's crust.

Two major forms of silicates exist in the earth's crust, namely: crystalline and non-crystalline forms. The most common form of crystalline silicate is quartz (Aydinap, 2012), which represents the second most common mineral in the earth's crust.

The material used in this study was quartzite rock, which is predominately comprised of the mineral quartz.

2.1.2 Quartzite rock

Quartzite rock (Figure 2.1) is a metamorphic rock that is formed when quartz-rich sandstone is exposed to high temperature and pressure, usually caused by tectonic compression. Quartzite generally comprises more than 90% quartz. Pure quartzite is usually white, but it can exhibit a variety of colors, as a consequence of incorporating other elements during metamorphosis.

Figure 2.1: Sample of quartzite rock

Source: King (2005)

2.1.2.1 Characterization of quartzite:

Perrone and Finlayson (2014) defined XRF spectrometry as a "non-destructive method of elemental analysis". They describe how the surface of the sample to be analyzed is bombarded

by primary X-rays, which causes secondary fluorescent X-rays to escape from the sample, and which are measured by the detector of the spectrometer. The detector is connected to a computer which is used to interpret the information, so as to characterize the elements in the sample. (See Figure 2.2.)

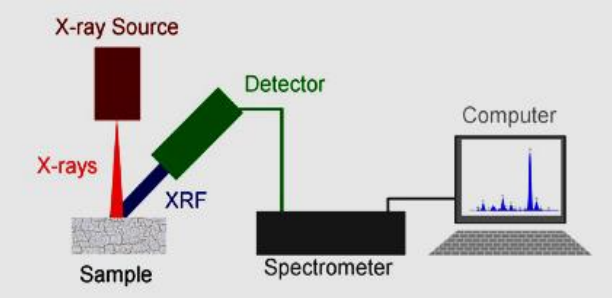

Figure 2.2: X-Ray Fluorescence Analysis principle

Source: Garba et al. (2013)

Singh et al. (2017) collected samples of quartzite rocks from different locations in parts of the Nalgonda district in India. The samples were subjected to petro-mineralogical and geochemical analysis (XRF). As expected, the results for all the samples indicated a high percentage of SiO_2 (83.31-98.67 wt%). For illustration purposes, the detailed results for three samples are shown in Table 2.1.

Table 2.1: Major oxide (wt%) data of quartzites from the Srisailam, Banganapalle and Paniam formations.

Sample No.	SiO_2	TiO_2	Al_2O_3	Fe_2O_3	MgO	MnO	CaO	Na_2O	K_2O	P_2O
PI/14/KGF /1A/306.05	83.65	0.21	6.40	1.39	0.98	<0.01	0.26	<0.01	5.66	0.09
PI/14/KGF /1A/359.05	98.60	0.04	0.01	0.26	0.14	0.01	0.31	<0.10	0.10	0.05
PI/14/RCH /2/311.25	68.44	0.63	14.21	4.00	3.38	0.01	0.13	<0.01	8.97	0.15

Source: Singh et al. (2017)

2.1.2.2 Uses of quartzite

Quartzite is very common and has a wide range of uses. It is used for roof and floor tiles and as a decorative stone for wall cladding. Crushed quartzite is used in road construction and for railway ballast. High purity quartzite is used to produce industrial silica, silicon and silicon carbide (Elzea et al, 2006). Some other uses that have been explored recently and are described below.

Use in civil construction

Cabello et al. (2013) investigated the use of quartzite waste from quarries in the state of Minas Gerais, Brazil. They concluded that only one stage of crushing of quartzite would be needed to produce a material that is suitable for manufacturing pre-molded components.

Quartzite waste has also been used to produce Reactive Powder Concrete (RPC) which presents high compressive strength in civil construction. For instance, Junior et al. (2019) used the tailings wastes produced by quartzite mining at Minas Gerais in Brazil, to produce RPC. Their work showed good behavior of quartzite with compressive strength between 85 MPa and 143 MPa.

Use in manufacturing refractory silica bricks

Hussein et al. (2017) considered manufacture of refractory silica bricks from quartzite rocks by comparing their properties with the required specifications. He concluded that a tunnel kiln could be used for this purpose, with a firing period of not less than 12 days.

2.2 Comminution

Gupta and Yan (2006) state that, depending on the host rock's characteristics, two methods are employed to extract ores of commercial interest, namely: physical or chemical methods.

- Physical methods are typically used for soft host rocks and include the use of excavators, as illustrated in Figure 2.3.
- In contrast, chemical methods are used for hard host rocks, using blasting for example, as illustrated in Figure 2.4.

Most extracted ores are in form of large rocks called “Run of Mine” (ROM). The ROM is physically composed of an association of both minerals with no economic value (gangue) and minerals of interest.

Comminution is the term used to describe the process and study of detaching or liberating the minerals of interest from the non-valuable ones using size reduction (Gay, 2004). The origin of the word “comminution” is the Latin word "comminuere", which means "to make small" (Gupta and Yan, 2006). Comminution operations are very energy-intensive, and they use up to 70% of the total expended energy in the mining industry (Rozenbaum et al., 2016). Therefore, optimising the process of mineral liberation, so as to reduce energy and maximize recovery of the mineral, is crucial.

According to Gupta and Yan (2006), the product particle size at which the maximum amount of mineral of interest is liberated from the host rock is called the liberation size. Therefore, the purpose of comminution is to optimize the breakage of the material of interest into this liberation size.

Figure 2.3: Excavator.

Source: Atherton (2017)

Figure 2.4: Blasting.

Source: Mining for Zambia (2016)

Wills (1985) explains that in order to achieve the breakage of material into the liberation size, a sequence of crushing and grinding processes are performed. Crushing the ROM material reduces the average particle size so that it is suitable as a feed for grinding. Grinding further reduces the PSD, until the mineral of interest is detached or liberated from the gangue.

2.2.1 Crushing

Mosher (2016) defines crushing as generally being a dry operation of size reduction of the ROM that is performed by compressing or impacting the material against rigid surfaces of the equipment (the crusher). He further states that crushing is generally realized in two stages, using specific crushers: primary and secondary crushing.

Pryor (1965) explains that, at the stage of primary crushing, the ROM material is reduced to a maximum size of 10 to 15 cm average diameter. In contrast, the secondary crushing receives material of less than 15 cm and reduces the size of the particles to below 2 cm.

2.2.1.1 Primary Crushers

Primary crushers are used to handle dry ROM rocks and are heavy-duty machines that are categorized into two main types, namely, gyratory crushers and jaw crushers (Fuerstenau and Han, 2009).

Jaw crusher

A jaw crusher is a compression crusher designed for large scale crushing operations (Kelly and Spottiswood, 1982). Gupta and Yan (2006) explain that the design of a jaw crusher is such that it has two surfaces made of hardened steel, called jaws. The two surfaces are oppositely inclined to form a V-shaped crushing zone. (See Figure 2.5.) One jaw is movable (called the swing jaw), whereas the other is fixed. The swing jaw can be spun either at the top-end, as in the Blake crusher, or the bottom end, as in the Dodge-type crusher. The movement of the pivoted jaw is caused by the toggle. (See Figure 2.5.) The swing jaw's retrieving movement is created by springs in small crushers or a Pitman in larger crushers. Both jaws of the crusher could be flat, or the fixed jaw could be flat and the mobile jaw convex. Furthermore, the surface of both jaws could be either smooth or corrugated (Gupta and Yan, 2006).

According to Deniz (2011), the material charge is fed into the crushing zone through an upper opening. The swing jaw conveys the force of the impact on the particles detained against the fixed jaw. Consequently, the material is crushed into smaller sizes and slides down into the V gap (Figure 2.5). The operation is repeated until the particle size is less than that of the bottom gap and, the material therefore passes through into the chamber as the product.

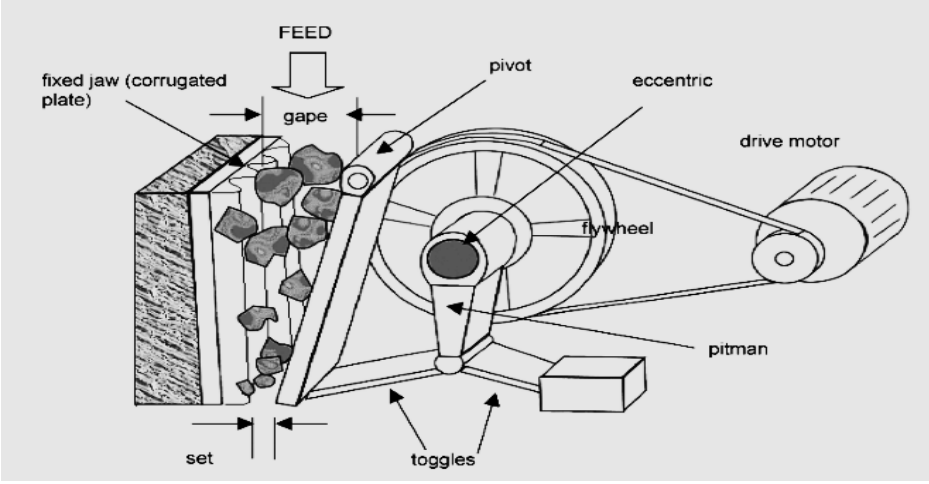

Figure 2.5: Jaw crusher design.

Source: Reprinted from "Mineral Processing, Design and Operations, second edition" (p100) by A. Gupta and D.S. Yan (2006). Elsevier. Copyright© 2006 by Elsevier B.V. Reprinted with permission.

Gyratory crusher

The gyratory crusher was invented in 1877 by Charles Brown and modified and further developed in 1881 by Gates (Gupta and Yan, 2006). The smaller version of a gyratory crusher is called a cone crusher. It is used for secondary crushing. Larger gyratory crushers are designed for primary crushing and reduce the size by a maximum of about one-tenth.

Gupta and Yan (2006) describe gyratory crushers as having a fixed solid conical shell or bowl and a solid cone within the bowl, called the breaking head, which is fixed to a central spindle. The central spindle is hydraulically suspended or mechanically held by a spider, and it generally rotates between 85 and 150 rev/ min. (See Figure 2.6.) The crushing is performed by the movement of the mantle or conical head that squeezes the charge of material against the concave shell or bowl. (See Figure 2.7.) The crushed material slips down by means of gravity when the mantle moves away during its cycle of gyration, and, with the next cycle, the crushed material is again caught between the mantle and the concave shell or bowl, resulting in further breakage. The operation is repeated until the size of the crushed material is less than the opening at the bottom, and the material flows out of the crusher.

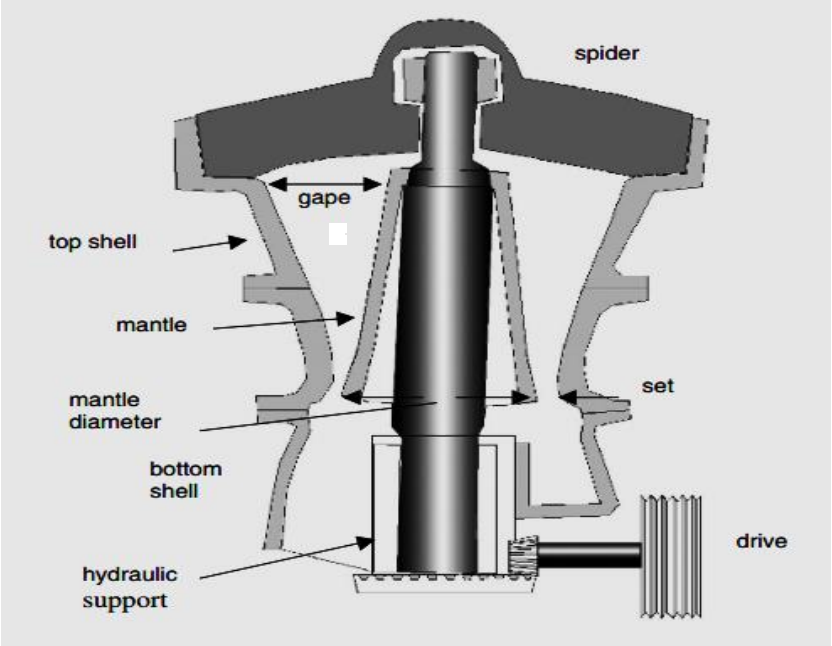

Figure 2.6: Sketch of a gyratory crusher.

Source: Reprinted from "Mineral Processing, Design and Operations, second edition" (p129) by A. Gupta and D.S. Yan (2006). Elsevier. Copyright© 2006 by Elsevier B.V. Reprinted with permission.

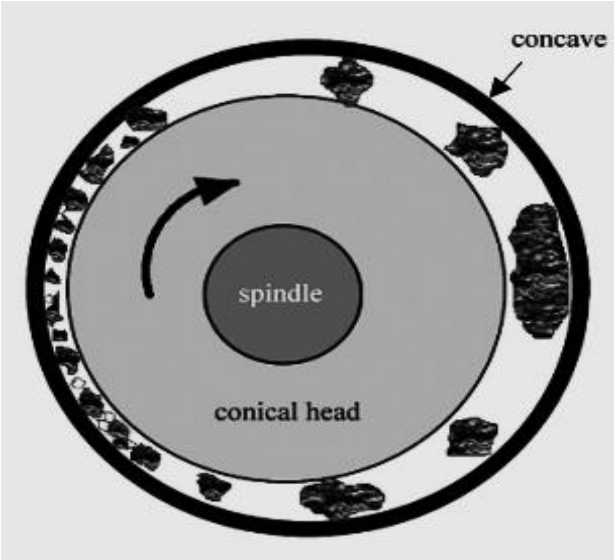

Figure 2.7: Section of a gyratory crusher.

Source: Reprinted from "Mineral Processing, Design and Operations, second edition" (p130) by A. Gupta and D.S. Yan (2006). Elsevier. Copyright© 2006 by Elsevier B.V. Reprinted with permission.

2.2.1.2 Secondary crushing

Secondary crushers treat the product produced by the primary crusher. Secondary crushers are much lighter than primary crushers, and the maximum feed size to these crushers is usually less than 15 cm in diameter (Pryor, 1965).

The purpose of secondary crushing is to reduce the size of the material produced by the primary crushing to a suitable size for grinding. Wills (1985) states that, in some cases, where the grinding feed size requirement is not satisfied by secondary crushing, a tertiary stage, called tertiary crushing, may be recommended, before the material is passed to the grinding stage.

There are three main types of secondary crushers: a cone crusher; a hammer mill; a roll crusher.

Cone crusher

The cone crusher is a modified gyratory crusher (Wills, 1985). It has a shorter spindle that is supported on a curved bearing below the cone, but which is not suspended, as in the gyratory crusher. (See Figure 2.8.) The opening of the crushing zone decreases from top to bottom, forcing a reduction of particle size as the material moves through the device.

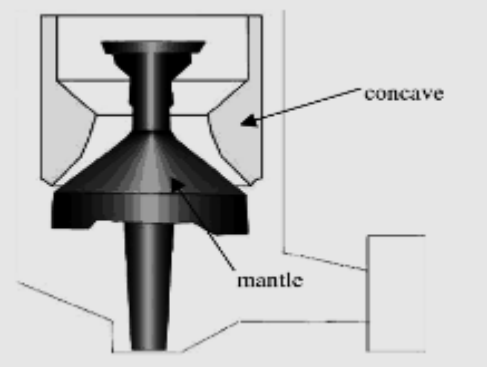

Figure 2.8: Cone crusher.

Source: Reprinted from "Mineral Processing, Design and Operations, second edition" (p131) by A. Gupta and D.S. Yan (2006)., Elsevier. Copyright© 2006 by Elsevier B.V. Reprinted with permission.

Hammer mill

A hammer mills break material by the impact of the rotating hammers on the material in the crushing zone, as illustrated in Figure 2.9. Wills (1985) states that, unlike when the breakage of material is caused by pressure, which causes internal stresses in the material, impact crushing causes immediate fracture, with no residual stresses. This is valuable in construction materials. According to Fuerstenau and Han (2009), hammers are generally mounted on a horizontal rotating shaft or drum, as illustrated in Figure 2.9. The material is fed into the crushing zone, and the high-speed rotation of the rotor causes fracture of the material through the impact of the hammers on the material. Shredded material is expelled through screens at the bottom of the drum.

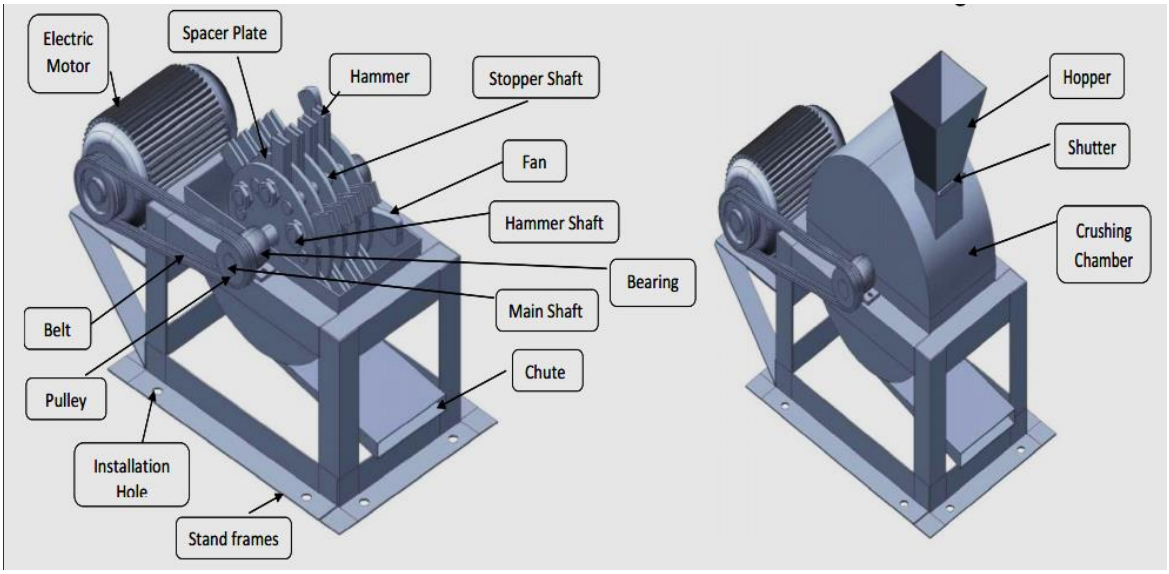

Figure 2.9: Sectioned and complete views of hammer mill.

Source: Reprinted from "Development and Performance Evaluation of Improved Hammer Mill" by Nwadinobi Chibundo Princewill. (2017). Journal of Scientific and Engineering Research, 4(8), p160.

Roll crusher

Roll crushers have been used for more than 200 years and are classified according to the number of rolls (Swain et al, 2011). There are two major types of roller crushers, namely single and double roller crushers.

Single roll crusher

Swain et al (2011) state that the single roll crusher is one of the oldest primary crushers used, but it has lost popularity to jaw crushers and gyratory crushers because of the poor wear characteristics with hard rocks. They also describe the operating principles of a single roller crusher (Swain et al., 2011). As the feed material enters the crusher, some breakage occurs by the impact of the rotating roll on the material. Most of the breakage occurs when the material enters the crushing zone between the rotating roll and the stationary breaker. Breakage occurs due to shearing forces between the rock and the teeth on the roll. Crushed material slips down through the discharge end of the crusher, as illustrated in Figure 2.10.

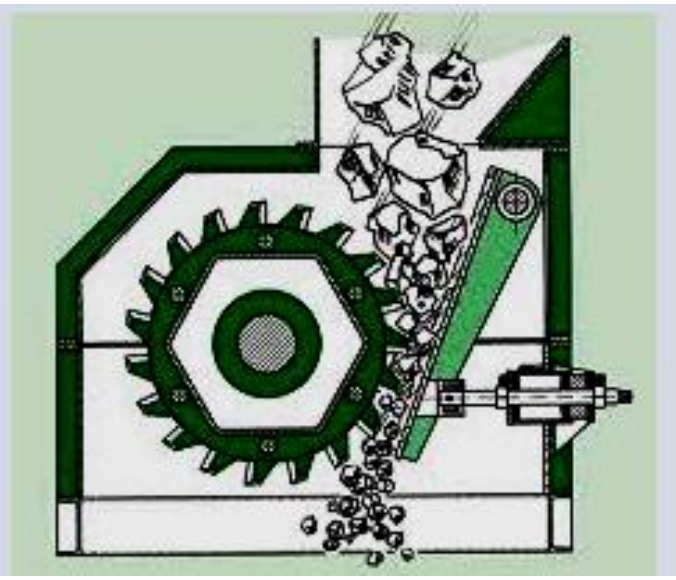

Figure 2.10: Single roll crusher.

Source: AUBEMA (2020)

Double roll crusher

Double roll crushers are composed of two adjacent heavy metal rolls, generally of the same diameter. The two rolls are supported by a shaft and placed parallel to each other, as illustrated in Figure 2.11. They rotate in opposite directions, and the rotating speed can either be the same or different (Swain et al, 2011). Roll crushers are fed from the top, and the material is nipped between the rolls and crushed by compression. After breakage, the crushed material is discharged from the bottom of the crusher.

Edmiston (2019) states that the characterization of a roller crusher is generally based on the following five elements: (1) configuration of the rolls (corrugated, smooth, or toothed); (2) size of the rolls (diameter of rolls, and width); (3) gap of the rolls; (4) rotating speed and (5) power. These characteristics are typically controlled during the design and operation of the mill, and are termed the mill operating conditions. In addition to these operating conditions, the final mill product size distribution also depends on the breakage characteristics of the material in the feed.

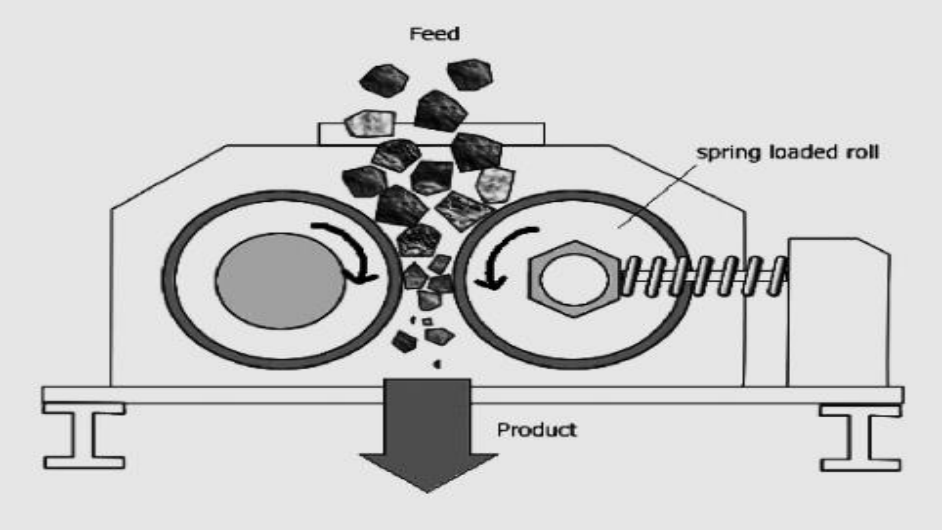

Figure 2.11: Smooth double roll crusher.

Source: Reprinted from "Mineral Processing, Design and Operations, second edition" (p143) by A. Gupta and D.S. Yan (2006) Elsevier. Copyright© 2006 by Elsevier B.V. Reprinted with permission.

2.2.2 Grinding

In many cases, crushing is not enough to liberate the mineral from the host rock or to obtain a product of the size of interest. Therefore, further size reduction (called grinding) of the crushed material is required. Tubular mills, as illustrated in Figure 2.12, or other devices, such as roller grinding mills (Figure 2.13 and Figure 2.14), are used to achieve this purpose.

2.2.2.1 Tubular mills

Gupta and Yan (2006) state that with tubular mills, grinding media, such as rods or steel balls are used to create a combined action of repeated impact and abrasion in the mixture during rotation of the mill. This repeat, combined action allows for progressive reduction in the size of material until the mineral is liberated.

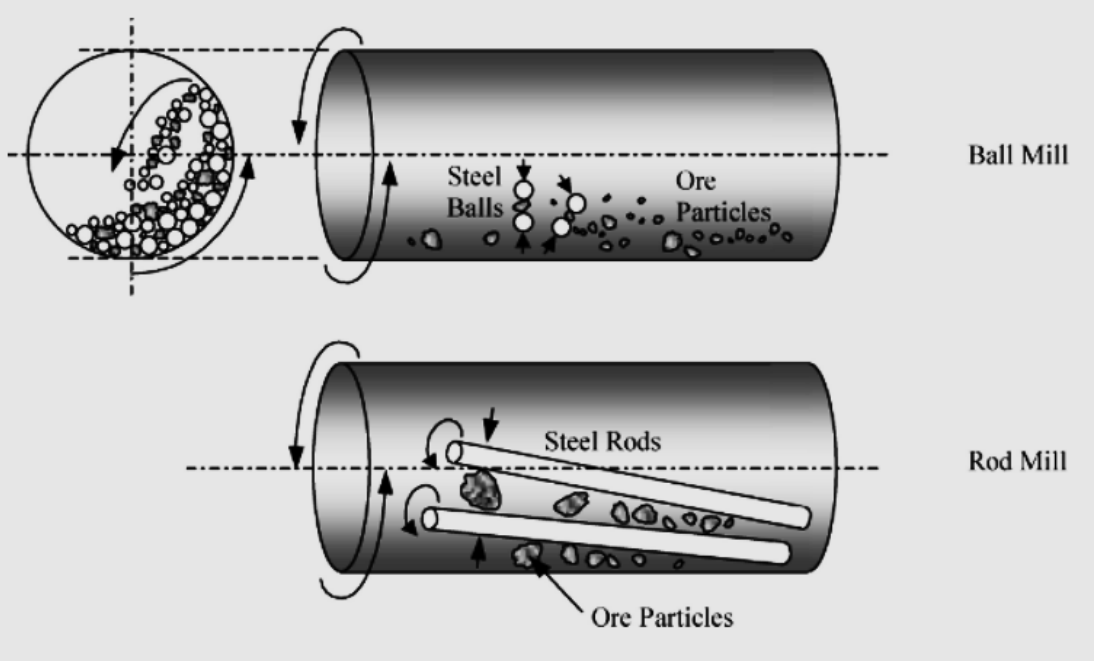

Figure 2.12: Mechanism of grinding in tubular mills.

Source: Reprinted from "Mineral Processing, Design and Operations, second edition" (p161) by A. Gupta and D.S. Yan (2006). Elsevier. Copyright© 2006 by Elsevier B.V. Reprinted with permission.

2.2.2.2 Roller grinding mills

The high-pressure grinding roll (HPGR) and the vertical roller mill (VRM) are the most frequently used roller grinding mills in minerals processing. These two technologies present some similarities and differences. They are both dry processes and break by compression in the same size range. However, their designs and operating conditions are different (Jankovic et al., 2016).

The HPGR consists of two motor-driven counter rotating rolls: one fixed, and one that moves laterally under pressure that is applied hydraulically. (See Figure 2.13). The material is choke-fed to the roll gap, and particles that are larger than the gap are nipped and broken to join particles that are smaller than the gap that are compressed in a bed formed between the rolls (Jankovic et al., 2016).

Reichert et al. (2014) state that in a VRM, the material is fed to the grinding table (Figure 2.14), where the centrifugal force moves it outward to be ground between the grinding elements (grinding table and rollers) and a particles bed is created. Afterward, particles are transported pneumatically above the grinding chamber, to a dynamic air separator for purposes of size classification. The coarse fraction is collected by the grid cone, while the fine fraction leaves the mill and enters a bag house.

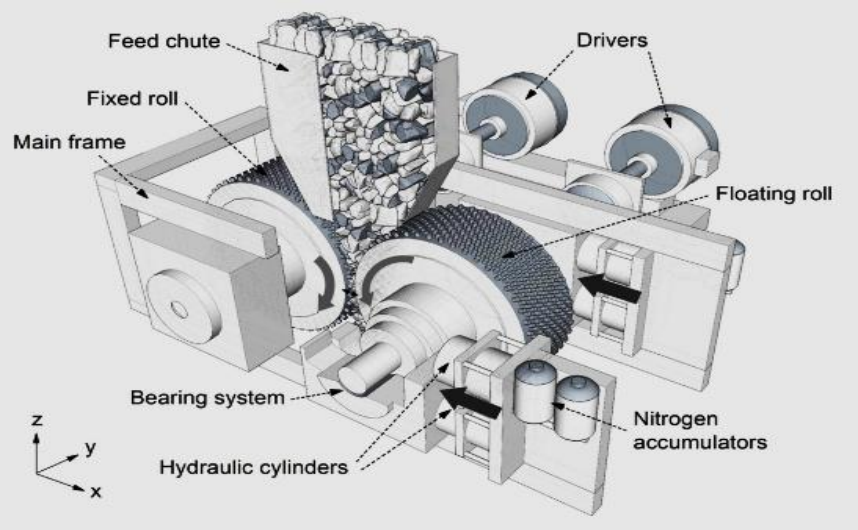

Figure 2.13. Schematic of the HPGR.

Source: Reprinted from "A preliminary model of high pressure roll grinding using the discrete element method and multi-body dynamics coupling" by G.K. Barrios and L.M. Tavares (2016). International Journal of Mineral Processing, p2, copyright© 2016 by Elsevier B.V. Reprinted with permission.

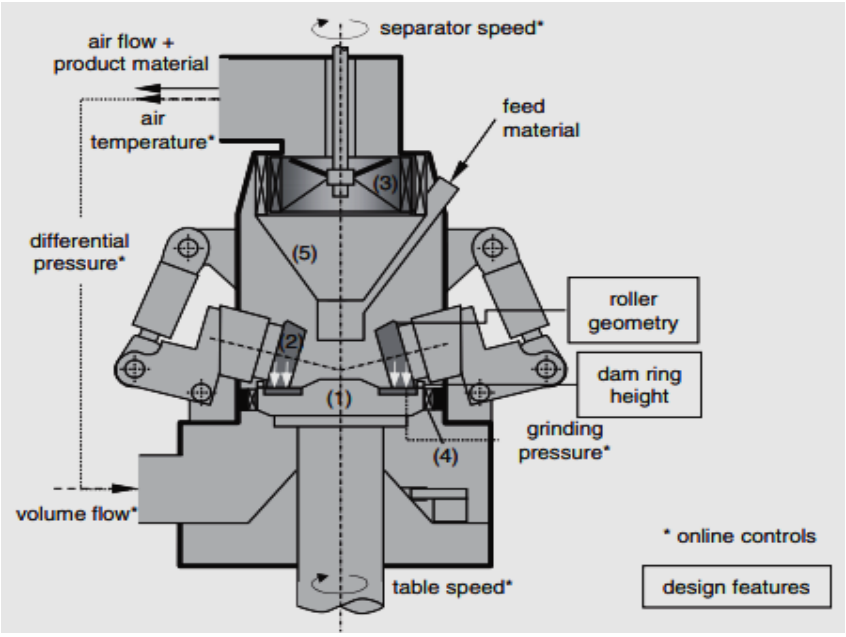

Figure 2.14: Schematic operation principle of a vertical-roller-mill.

((1) Rotating table. (2) Grinding track and rollers. (3) A dynamic air separator. (4) Louver ring. (5) E grid cone.)
Source: Reprinted from "Research of iron ore grinding in a vertical-roller-mill" by M. Reichert et al. (2014). Minerals Engineering, p2 copyright 2014 by Elsevier Ltd. Reprinted with permission.

Saravacos and Kostaropoulos (1928) state that some of the crushing and grinding equipment used in mineral processing can be adapted to food processing. They also report that with crushing and grinding roller equipment, the classification depends on the following factors: (1) type of size reduction; (2) size of end product; (3) reduction ratio; (4) main force applied. This is indicated in Table 2.2.

Table 2.2 Classification of food crushing and grinding roller equipment.

Type of size reduction	**Equipment**	**Size of end product**	**Reduction ratio (initial / final size)**	**Main force applied**
Stress between two rolls	Roll crusher	>10mm	4-6	Pressure and shear
	Roll mill	5µm-100µm	>20	

Source: Saravacos and Kostaropoulos (1928)

Therefore, it is clear that with either mineral processing or food processing, the term “mill” refers to a process of a high reduction ratio for finer product size.

2.3 Modeling in comminution

Modeling of comminution equipment is a description of the breakage process, using mathematical equations, so as to define the relationship between feed and product characteristics, including aspects such as the PSD, particle shape and the properties of the material. The mathematical equations are called models, as they can be used to optimize equipment or predict performance of comminution processes. The models are also employed for simulation purposes (Lynch and Morrison, 1999) and can be verified by comparing the predictions to experimentally measured data. In this study, the characterization of the material is limited to the size aspect only, as only one type of material was used in the experiments, namely quartzite.

According to Lynch and Morrison (1999), the initial research on defining a quantitative relationship between the energy consumed and the size reduction achieved in crushing and grinding was done by Rittinger (1867) and Kick (1883). In the process of size reduction, there is an increase in the surface area of the particles and Rittinger and Kick assumed that the energy of breakage is related to this increased surface area (Lynch and Morrison, 1999). Therefore, the difference in the surface area between the feed and product should be proportional to the energy consumed. The following relationship between the energy of the breakage process (E) and the surface area of the material (S) was proposed:

$$dE = k[S^n dS] \qquad \text{(Equation 2.1)}$$

Where: k is a constant and a function of the crushing strength of the rock;

n is a constant parameter, and according to different researchers, the value is:

n = -2 for Rittinger; n = -1 for Kick; n = -1.5 for Bond (Gupta and Yan, 2006).

Lynch and Morrison (1999) explain that the description of a PSD can frequently be simplified so as to be described by a single parameter, namely d50 or d80, which represents the size of the sieve through which 50% or 80% of the material passes, respectively. This simplified description of the PSD has, however, been found to be insufficient when modelling breakage mechanisms and therefore a PSD with two or more parameters is usually used.

In 1925, Paul Rosin and Erich Rammler proved that a simple negative exponential equation, with two parameters, could fit the PSD of crushed materials (Gupta and Yan, 2006); this is known as the Rosin Rammler distribution:

$$R = 100 \exp\left[-\left(\frac{x}{x^1}\right)^b\right] \qquad \text{(Equation 2.2)}$$

Where: R = cumulative mass % retained on size x;

x^1= size parameter;

b= distribution parameter.

2.3.1 Breakage function and breakage equation

The breakage equation is defined as "the mathematical relationship between feed particle size distribution and product particle size distribution" for given operating conditions (Campbell and Webb, 2001).

The probability density function (PDF) can be used to define the feed particle size distribution (PSD) to any milling system (Campbell et al., 2001). According to the ASCE (2008), the PDF is a mathematical formula with the form f(x), which allocates a non-negative value to any number x in the domain of the PDF. The integration of the PDF over the entire domain should yield a value of 1. A probability of between 0 and 1 results when integrating the PDF over a part of the domain.

The American Society of Civil Engineers (2008) goes on to state that the formula of the PDF can follow different trends or forms commonly used to describe probability distributions, including: (i) the normal or Gaussian distribution; (ii) the log-normal; (iii) the gamma and log-gamma distribution.

Campbell et al. (2001) state that if the PDF, $\rho_1(D)$, is applied to a PSD of some material, where D is a characteristic particle size (sieve size), the probability of a particle being in the size range $D \; to \; D \; + dD$, symbolized by $Pr\{D, D + dD\}$, is equal to $\rho_1(D)dD$. The probability of a particle in the material being smaller than D is defined as $F(D)$, and is given by:

$$F(D) = Pr\{0, D\} = \int_0^D \rho_1(D)dD \qquad \text{(Equation 2.3)}$$

The mass based PSD for the feed to a roller mill is denoted $\rho_1(x)$ and that of the product as $\rho_2(x)$. The breakage function, $\rho(\mathrm{x}, D)$, describes the relationship between $\rho_1(D)$ and $\rho_2(x)$, and is defined by:

$$\rho_2(x) = \int_{\mathrm{D=x}}^{D=\infty} \rho(\mathrm{x}, D)\rho_1(D)dD \qquad \text{(Equation 2.4)}$$

Campbell and Webb (2001) explain that $\rho(\mathrm{x}, D)$ represents the probability of producing a product particle of size x from a feed particle of size D. It is assumed that the product particles of size x cannot be created from the feed particles of size $D < x$. Therefore, the integration takes place over the range of feed particles for $D \geq x$. Equation (2.4) is known as the breakage equation.

2.3.2 Breakage matrix

Broadbent and Callcott (1956) used a cone crusher to mill coal, which they considered to be a homogenous rock. They assumed that the breakage of particles can be described by two processes, namely: (i) selection of particles to be broken; (ii) breakage of the selected particles. The aim of the study was to describe a method of defining both the selection and breakage functions for a milling process. They concluded that a matrix form could be successfully used to define both the selection function and the breakage function.

Campbell et al. (2001) demonstrated that the discretization of the breakage equation (equation 2.5) gives a matrix form (equation 2.5), which can be used to predict the product size distribution for roller milling of wheat. If the feed PSD is discretized into n size classes, we can define the feed vector as **f** = (f_1, f_2, …f_n), where f_i is the mass fraction of feed material of size i. Similarly, if the product PSD is discretized into *m* size classes, the product PSD is described by the product vector **o** = (o_1, o_2, … o_m), where o_i is the mass fraction of product of size i. The relationship between **f** and **o** is given by:

$$\begin{bmatrix} b_{11} & b_{12} & \ldots\ldots & b_{1n} \\ b_{21} & b_{22} & \ldots\ldots & b_{2n} \\ . & . & . & . \\ . & . & . & . \\ . & . & . & . \\ b_{m1} & b_{m2} & . & b_{mn} \end{bmatrix} \times \begin{bmatrix} f_1 \\ f_2 \\ . \\ . \\ . \\ f_n \end{bmatrix} = \begin{bmatrix} o_1 \\ o_2 \\ . \\ . \\ . \\ o_m \end{bmatrix} \qquad \text{(Equation 2.5)}$$

$here$: b_{ii} is the mass fraction of material retained on sieve i from the milling of a single particle size or narrow size i;

b_{ij} is the mass fraction of material retained on sieve i from the milling of a single particle or narrow size j.

We define the breakage matrix ***B*** to be a matrix of m rows and n columns with elements b_{ij}, where $0 \leq i \leq m$ and $0 \leq j \leq n$. Equation 2.5 can then be written as:

$$\mathbf{B}f = 0 \qquad \text{(Equation 2.6)}$$

The vectors **f** and **o** represent the discretized feed and product PSD, respectively. Therefore, the sum of their fractions must equal unity or:

$$\sum_{j=1}^{n} f_j = 1 \qquad \text{(Equation 2.7)}$$

$$\sum_{i=1}^{m} o_i = 1 \qquad \text{(Equation 2.8)}$$

In order for equation (2.8) to be satisfied, it can be shown that:

$$\sum_{i=1}^{m} b_{ij} = 1 \text{ for all j, such that } 0 \leq j \leq n \qquad \text{(Equation 2.9)}$$

Campbell and Webb (2001) showed that the elements of the breakage matrix are related to the breakage function by:

$$b_{ij} = \frac{1}{D_{j-1} - D_j} \int_{D_j}^{D_{j-1}} \int_{x_{i-1}}^{x_i} \rho(x, D) dx dD \qquad \text{(Equation 2.10)}$$

2.3.3 Normalizable and non-normalizable breakage matrices

According to Gupta and Yan (2006), if standard sieves are arranged in a geometric manner ($1/\sqrt{2}$ series) and no agglomeration occurs, two classes of the breakage matrix can be defined: normalized and non-normalized. A breakage matrix is normalized when two conditions are satisfied: (i) the milling of various feed sizes produces a superposition of size distributions in the product; (ii) the breakage function describes or fits the superposition of size distributions. If the breakage matrix is normalizable, the matrix (equation 2.5) becomes a diagonal matrix, as illustrated in equation (2.11):

$$\begin{bmatrix} b_{11} & 0 & \dots & 0 \\ b_{21} & b_{11} & \dots & 0 \\ b_{31} & b_{21} & \dots & 0 \\ . & b_{31} & \dots & . \\ . & . & \dots & . \\ b_{m1} & b_{(m-1)1} & \dots & b_{11} \end{bmatrix} \qquad \text{(Equation 2.11)}$$

The breakage function is non-normalized if there is variation of product size distribution with respect to the feed size.

2.3.3.1 Examples of normalized breakage functions

Various authors have developed different forms of normalized breakage functions. The various approaches and the resulting breakage functions are discussed below.

Klimpel and Austin (1977)

The process of fragmentation of brittle materials in a mill is considered to occur in two steps: first the crack initiation from inside the particle, and second the crack propagation through the particle (Weichert, 1988). Originally, the description of the initiation of the fragmentation process was done using Weibull statistics. However, this was found to be insufficient to describe the complete fragmentation process. Klimpel and Austin (1977) extended the Weibull statistics using equation (2.12) to describe the complete fragmentation process.

$$B(x_i) = 1 - \left[1 - \left(\frac{x_i}{x_j}\right)\right]^{n_1} \left[1 - \left(\frac{x_i}{x_j}\right)^2\right]^{n_2} \left[1 - \left(\frac{x_i}{x_j}\right)^3\right]^{n_3} \qquad \text{(Equation 2.12)}$$

Where: x_j = the initial size being broken:

x_i = the size of the fragment after breakage;

n_1-n_3 = the constants, depending on the particle shape;

$B(x_i)$ = the cumulative mass fraction finer than $x_j > x_i > 0$.

Broadbent and Callcott (1956)

Coal was separated into different particle sizes and milled using a cone mill. For each particle size, equation (2.13) could be used to describe the product PSD. This is shown in Figure 2.15.

$$B(x,y) = \frac{\left[1-\exp\left(-\frac{x}{y}\right)\right]}{[1-\exp(-1)]}, 0 < x \leq y \qquad \text{(Equation 2.13)}$$

Where: $B(x,y)$ is the proportion by weight of the product that has a size of less than x;

y is the size of the original particle, where the size is determined by sieving.

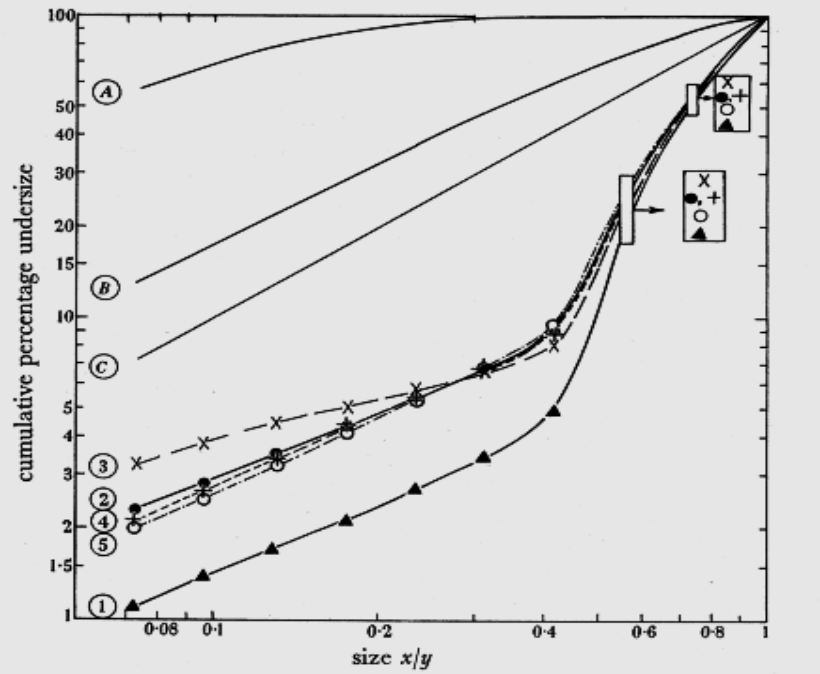

Figure 2.15: Comparison of three breakage functions.

Product from the breakage of single particles:

$\mathbf{A, B}\left(\frac{\mathbf{x}}{\mathbf{y}}\right) = \mathbf{1} - \mathbf{exp}\left(-\frac{\mathbf{10x}}{\mathbf{y}}\right)$**;** $\mathbf{B, B(x, y)} = \frac{\left[\mathbf{1-exp}\left(-\frac{\mathbf{x}}{\mathbf{y}}\right)\right]}{[\mathbf{1-exp(-1)}]}$**;** $\mathbf{C, B}\left(\frac{\mathbf{x}}{\mathbf{y}}\right) = \mathbf{x/y}$ **; 1 feed to cone mill**

Source: Broadbent and Callcott (1956)

Austin et al. (1984)

Different materials, including quartz, were milled in a ball mill under various mill load conditions. For some materials, the resulting cumulative size distributions of the product fell on top of one another, despite the use of various feed sizes. An empirical function that is given in equation (2.14), could describe the breakage.

$$B_{i,j} = \emptyset_j \left(\frac{x_{i-1}}{x_j}\right)^{\gamma} + (1 - \emptyset_j)\left(\frac{x_{i-1}}{x_j}\right)^{\beta}, 0 \leq \emptyset_j \leq 1 \qquad \text{(Equation 2.14)}$$

Where: $B_{i,j}$ = fractions of particles finer than size i from the breakage of the particle of size j

γ is the slope of the lower section of the Bi,j curve;

β is the slope of the steeper section of the Bi,j curve;

$\emptyset_j$ is the intercept at $\frac{x_{i-1}}{x_j} = 1$.

This is illustrated in Figure 2.16.

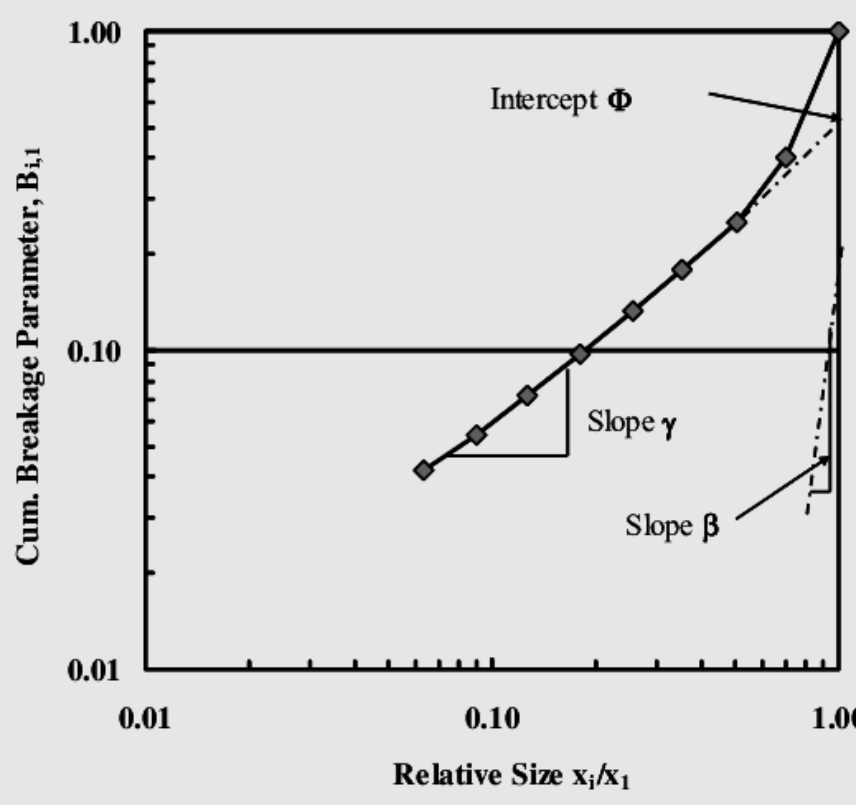

Figure 2.16: Primary breakage particle size distribution function parameters for any single size fraction feed ground in a ball mill.

Source: Austin et al. (1984)

Austin et al. (1984) also assert that γ, β, and $\emptyset_j$ are found to be material-dependent and are called parameters of the breakage distribution function.

2.3.3.2 Example of the non-normalized breakage function

According to Austin et al. (1984), the primary progeny fragment distributions for larger sizes in ball milling sometimes have different B values (corresponding to a non-normalized breakage

function). Equation (2.14) was modified empirically to account for this and delivers equation (2.15):

$$B_{i,j} = \emptyset_j \left\{ \frac{1-exp\left[-\left(\frac{\frac{x_{i-1}}{x_j}}{k}\right)^{\gamma}\right]}{1-exp\left[-\left(\frac{1}{k}\right)^{\gamma}\right]} \right\} + \left(1-\emptyset_j\right)\left(\frac{x_{i-1}}{x_j}\right)^{\beta} \qquad \text{(Equation 2.15)}$$

Where: k is an additional parameter that fits the finer sizes to the Rosin-Rammler distribution.

Austin et al. (1984) also state that, in their experience, the assumption of normalized breakage function is not correct for ball milling of brittle materials in most cases. Therefore, a false assumption could cause significant errors and complexity in the analysis of experimental data.

2.3.4 Modeling in roller milling

Austin et al. (1980) separated coal into five narrow sizes, using geometric intervals ($\sqrt{2}$ size intervals). They used these geometric intervals on the assumption that particles should break independently of one another (Austin et al., 1980). The narrow sizes were milled using a laboratory smooth double roller mill with a 1.68 mm gap size. The PSD of the product was plotted as shown in Figure 2.17, and the cumulative fraction passing was obtained using equation (2.17).

$$\overline{B_{i,J}} = \sum_{k=i}^{n} \overline{b_{k,J}} \qquad \text{(Equation 2.16)}$$

Considering that each narrow size is represented by the mean size (the size midway between the upper sieve and the lower sieve size), when a narrow size of mean size j passes through the mill, the weight fraction retained on sieve size i in the product is $\overline{b_{k,J}}$. (The overbar means that this product fraction retained is related to the mean size explained above.) Austin et al. (1980) state that it is easiest to determine the values of $\overline{b_{k,J}}$ by working from the bottom size up, to get the cumulative fraction passing the upper sieve size i.

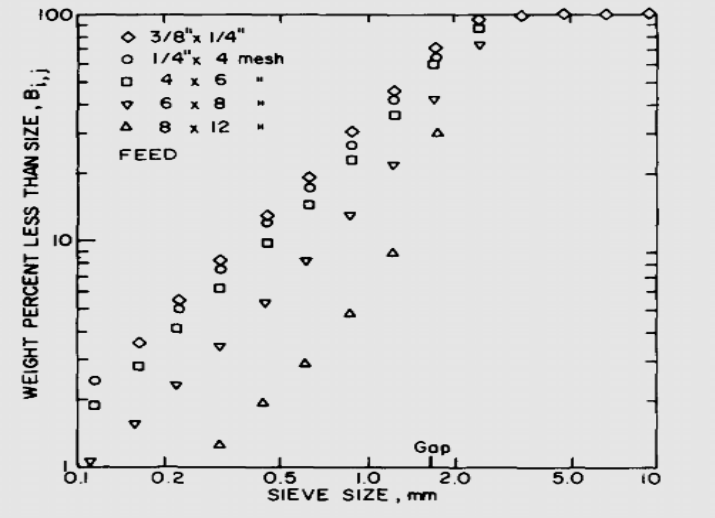

Figure 2.17: Size distribution from various feed sizes of coal through a 12-mesh gap size.

Source: Austin et al. (1980)

Austin et al. (1980) also state that the milling ratio does not affect the product size distribution, as illustrated in Figure 2.18. Therefore, the normalized breakage function described in equation 2.15 could fit the cumulative product size distribution.

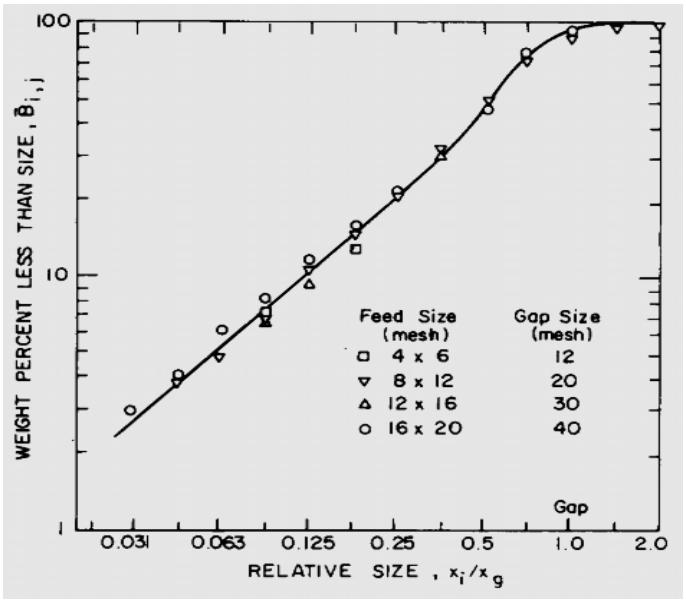

Figure 2.18: Product PSD for various feed and gap sizes.

The term x_j/x_g is the milling ratio.

Source: Austin et al. (1980)

Rogers and Shoji (1983) used the procedure suggested by Austin et al. (1980) to determine the breakage parameters for roller milling of coal and thereby developed a predictive model. The sieving error $\in_s$ was determined by repetitive sieving of each narrow size sample without crushing. The sieving error is the fraction smaller than the initial narrow size obtained after repeating the sieving.

Using a gap size of 1.68 mm, feed samples of different narrow sizes were fed separately into the mill. The product size distribution was determined and used to estimate the model parameters for coal, as illustrated in equation 2.15.

$$a_i = 1 - \frac{p_i}{1-\in_s} \qquad \text{(Equation 2.17)}$$

Where: a_i is the primary bypass parameter for each narrow size fed into the mill;

p_i is the weight fraction in the product, which is retained within the feed size interval.

After plotting graphs of bypass versus product size distribution, it was found that interpolation and extrapolation could be done using equation 2.18.

$$a_i = 1 - \frac{1}{1+\left(\frac{x_i/x_g}{\mu}\right)^{\lambda}} \qquad \text{(Equation 2.18)}$$

Where:

x_g is the gap size in millimeters;

λ and μ are fitted parameters.

The values were found to be $\lambda = 6.6$ and $\mu = 1.6$ for the breakage of coal in this research.

The modeling of roller mills follows one of two approaches: firstly those who used the procedure suggested by Austin et al. (1980) to model the milling; and secondly those who followed the

matrix approach initiated by Broadbent and Callcott (1956). This matrix approach was used by Campbell et al. (2001) for roller milling of wheat grain.

Campbell et al. (2001) prepared five samples of different size fractions of wheat grain, using geometric intervals. After being conditioned to 16% moisture overnight, each sample was milled in a test roller mill. The rolls were fluted and rotated at a differential of 2.7 relative to a fast roll speed of 600 rpm. Using ten different roll gap settings, covering 0.05 mm increments over 0.25-0.7 mm, samples were milled at a feed rate corresponding to 375-500 kg/ hr. Assuming that particles break independently on one another, the product fraction retained from the sieve analysis was used to construct a breakage matrix for each gap size. The breakage matrix was then used to predict the product size distribution for any feed.

It was found that the product PSD depended critically on the milling ratio illustrated in Figure 2.19. In addition, the breakage function was found to be non-normalized, as the feed size affected the size distribution of the product. Equation 2.19 was used to describe the breakage function, where the breakage function is linear in x.

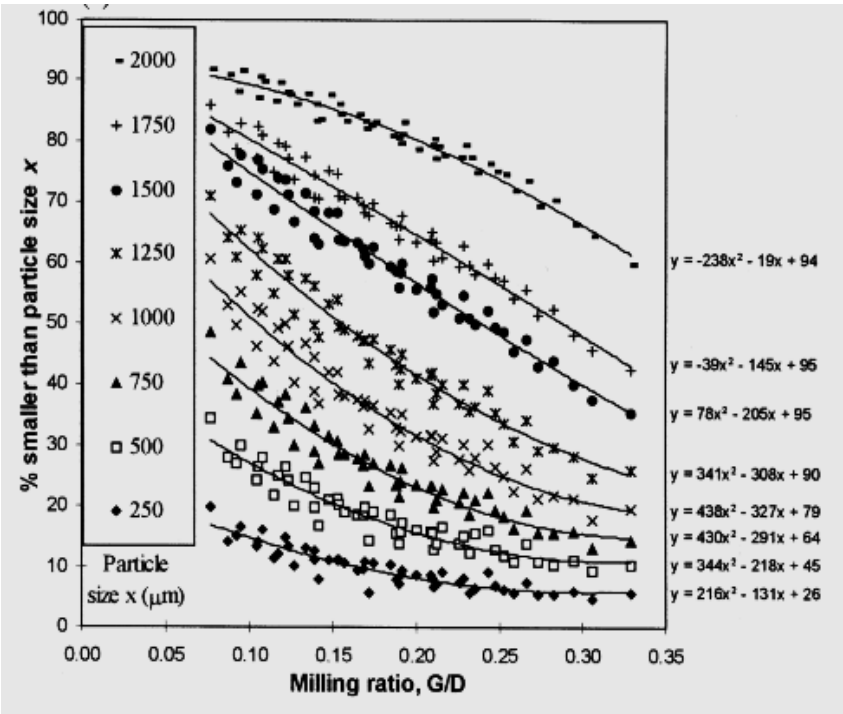

Figure 2.19: Product cumulative size distribution versus milling ratio.

Source: Campbell et al. (2001)

$$\rho(x,D) = [1 \quad (G/D) \quad (G/D)^2] \begin{pmatrix} b_o & 2c_0 \\ b_1 & 2c_1 \\ b_2 & 2c_2 \end{pmatrix} \begin{bmatrix} 1 \\ x \end{bmatrix} \qquad \text{(Equation 2.19)}$$

The proportion of particles of size x varies as a quadratic function of the milling ratio (G/D). The b coefficients represent the variation in the intercept of the breakage function, while the milling ratio and the c coefficients describe the variation of the slope.

Fistes et al. (2013) used the breakage matrix approach to determine the optimal feed size distribution of wheat grain, in order to achieve a desired product PSD. They used the system of linear equations illustrated in equation 2.20 to rewrite equation 2.5 as follows:

$$(b_{11} - b_{1n})f_1 + (b_{12} - b_{1n})f_2 + \cdots + (b_{1n-1} - b_{1n})f_{n-1} = o_1 - b_{1n}$$

$$(b_{21} - b_{12})f_1 + (b_{22} - b_{2n})f_2 + \cdots + (b_{2n-1} - b_{2n})f_{n-1} = o_2 - b_{2n}$$

….

$(b_{m1} - b_{mn})f_1 + (b_{m2} - b_{mn})f_2 + \cdots + (b_{mn-1} - b_{1m})f_{n-1} = o_m - b_{mn}$ (Equation 2.20).

The approach suggested by Austin et al (1980) for roller milling of coal set a certain boundary on product particle size (less than 400 mesh) for modeling in order to use the assumption of normalization. They also state that there is a shift from normalized to non-normalized breakage distribution when considering larger product particles. In contrast, the approach used by Campbell et al. (2001) for roller milling of wheat grain does not present any limitation in the product particle size for modelling. Therefore, this latter approach was adopted in this study on roller milling of quartz.

Chapter 3: Materials and Methods

This chapter presents the equipment, the materials used and the tests performed in the laboratory, in order to achieve the objectives defined for this study. The laboratory tests were conducted at the Mineral Processing Laboratory at the University of Johannesburg, Doornfontein Campus, in the Republic of South Africa. The material used in this study was quartzite rock.

This chapter is divided into two sections. The first section focuses on the preparation of narrow sizes of the material and describes the jaw crusher equipment used for the primary crushing of the blocks of quartzite. The methods and equipment used for sieving are also described. The second section describes the roller milling procedure used on the narrow sizes product generated by the jaw crusher and the sieve analysis of the roller milling product, which led to the construction of the breakage matrices. The experiments that were performed to validate the models developed in this work are also described in the second section.

3.1 Preparation of narrow sizes

3.1.1 Materials

Eighteen blocks of quartzite rocks were used as the source material for the experiment. The shape of the as-received blocks of quartzite was irregular, as illustrated in Figure 3.1. The blocks weighed 7 kg on average. The X-Ray Diffraction Analysis for elemental composition was performed by the analytical department of the University of Johannesburg. The results show that SiO_2 is predominant element in all samples. See Table 3.1.

Figure 3.1: Sample of quartzite rocks.

Table 3.1: Elemental composition of the material (quartzite) using X-Ray Diffraction Analysis.

Component	Unit	Result
Na_2O	mass %	0.6821
MgO	mass %	0.172
Al_2O_3	mass %	7.7049
SiO_2	mass %	86.8477
P_2O_5	mass %	0.0301
SO_3	mass %	0.3767
Cl	mass %	0.0617
K_2O	mass %	1.5943
CaO	mass %	0.2486
TiO_2	mass %	0.2293
V_2O_5	mass %	0.0211
Cr_2O_3	mass %	0.177
MnO	mass %	0.0279
Fe_2O_3	mass %	1.7152
NiO	mass %	0.0294
CuO	mass %	0.0266
As_2O_3	mass %	0.0101
Rb_2O	mass %	0.0066
SrO	mass %	0.0146
ZrO_2	mass %	0.0243

3.1.2 Jaw crushing

The blocks of quartzite were crushed in a jaw crusher with corrugated jaws. (See Figure 3.2.) The crusher has a 120 mm fixed opening side, 12 mm closing set, and is 400 mm wide. Crushing was

performed at 3273 rpm, with a feed rate estimated to be 14 kg/min. The blocks of quartzite were dropped one a time into the crusher, as illustrated in Figure 3.2. Crushing time for each block was estimated to be 30 seconds, on average.

Safety precautions were taken during process of crushing the blocks of quartzite rock.

After cleaning the crushing circuit, a collecting bucket was placed under the chute of the crushing circuit, to collect and transport the Jaw crusher product. The blocks of quartzite rocks were dropped individually into the jaw crusher, before turning-on the conveyor belt and the crusher consecutively. The crusher was turned-on simultaneously with a chronometer in order to measure the crushing time of the block of quartzite. The completion of the crushing of a block of quartzite was detected from the drop of the breakage noise.

The crushed sample was then split using riffle splitters, as indicated in Figure 3.5. A sample holder was used to carry and drop a suitable amount of the material on to the riffle splitters. To ensure an equal distribution of the material on the rifle, a smooth and gradual inclination of the sample holder was done.

The jaw crusher product weighed 100 kg. After splitting, eight samples were produced, weighing approximately 12.5 kg on average.

Figure 3.2: Corrugated jaw crusher used for the experiments

Figure 3.3: Jaw crushing switch.

Figure 3.4: Jaw crushing circuit.

Figure 3.5: Splitting of jaw crusher product.

3.1.3 Jaw crusher product size analysis

The sieving was performed using an Analysette 3 Spartan sieve shaker using six square sieves with the following size openings (in mm): 18; 16; 13.3; 11.2; 8; 6.7. A collecting pan was also used. (See Figure 3.6.) Each 12.5 kg sub-sample was loaded onto the top sieve and sieved for 5 min using 3 mm amplitude on the sieve shaker. These settings were found to be optimum after a series of sieving tests were performed. The arrangement of sieves was geometric, as it was assumed that each size fraction should break independently of others (Austin et al., 1980).

Sieving was performed according to the Standard Test Method for Sieve Analysis of Fine and Coarse Aggregates (C136/C136M-14) (ASTM, 2015). The sieving process was repeated until each 12.5 kg sub-sample was split into six size classes, which were denoted A to F. This is shown in Table 3.2. These were then used as feed for the roller mill. The size distribution of the product from the jaw crusher is shown in Figure 3.8.

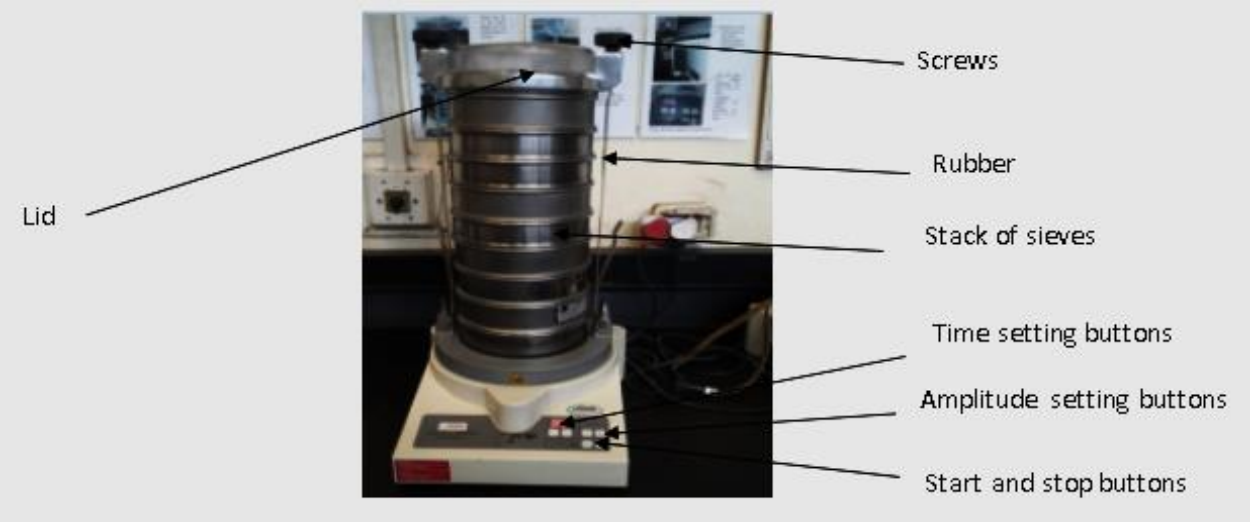

Figure 3.6: Sieving using a sieve shaker.

Figure 3.7: Samples of jaw crusher product after sieving.

Table 3.2: Details of size fractions produced from jaw crushing followed by sieving.

Jaw Crusher Product(g)	Size fraction range (mm)	Size Fraction Reference	Mass in Size Fraction (g)	Percentage of Size fraction (%)	Cumulative Passing Sieve Size (%)
100346	18-16	**A**	5017.3	5.00	95
	16-13,3	**B**	5368.5	5.35	89.65
	13,3-11,2	**C**	14048.4	14.00	75.65
	11,2-8	**D**	20069.2	20.00	55.65
	8-6,7	**E**	5458.8	5.44	50.21
	6,7-0	**F**	50383.8	50.21	0

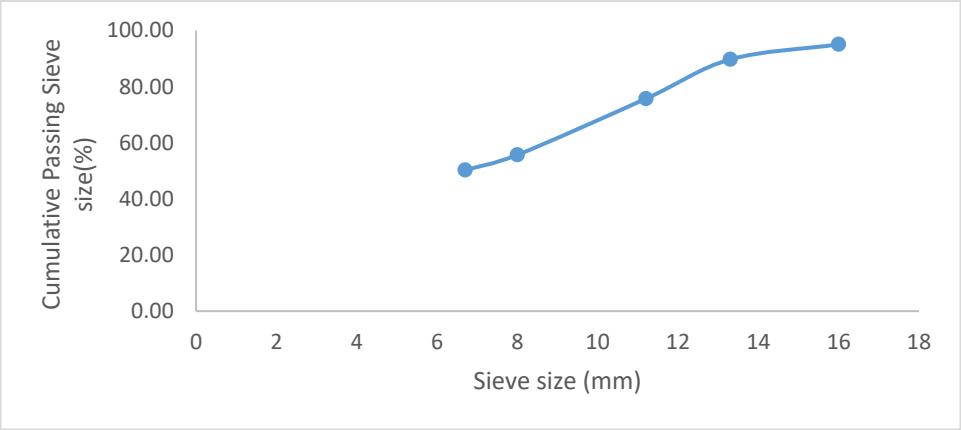

Figure 3.8: Size distribution of the jaw crusher product.

3.2 Roller milling of the narrow sizes and mixed feeds

The experiments performed on the roller mill are grouped into two sets, the first set comprise of milling of mono-sizes (Table 3.3) while the second set describes the milling of mixed feed (Table 3.4).

The material in the individual size fractions (A-F) were used as feed for the experiments on the roller mill. A Denver Colo 200x300 test double roller mill with smooth rolls (Figure 3.9) was used in these experiments. The roller mill was run at a fixed speed of 116 rpm, and three gap size (8, 10 and 12mm) settings were studied. The gap size was set on the mill and checked using a feeler gauge. The feeding of the roller mill was done slowly to avoid chocking of the crushing zone and the milling was done following the procedure outlined in section 3.2.1.

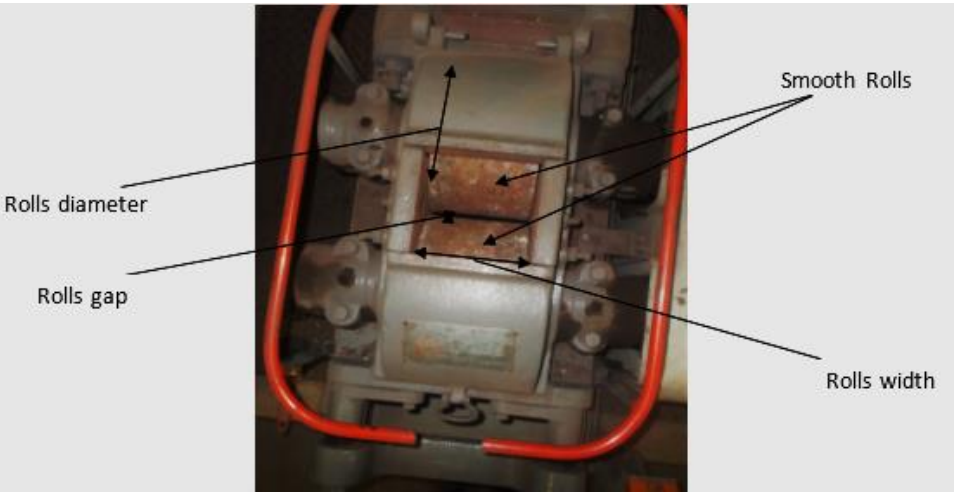

Figure 3.9: Roller mill

3.2.1 Roller milling procedure:

Several steps were taken during the roller milling of quartzite rocks. Initially, the rolls were cleaned using a brush to prevent any contamination of the material. Afterwards, the gap size was set using a specific feeler gauge. This preceded the installation of the hopper feeder on the roller mill, and the collecting bin under the mill.

The roller mill was then turn-on before the feeding of the material. A sample holder was used to carry the samples and feeds to the mill. The material was fed in such a way to avoid "chock feeding" or interactions between the particles.

Milling was repeated using different feed masses in each of the sizes classes i.e. (A to F) as indicated in Table 3.3 and labeled Test 1 and Test 2. These repeats were done to test the reproducibility of the milling as well as to assess the impact of feed mass in each size class on product size distribution.

Table 3.3: Feed masses used for the roller mill tests.
(Gap sizes are in mm.)

	Test 1				Test 2		
Fraction	**gap.8**	**gap.10**	**gap.12**		**gap.8**	**gap.10**	**gap.12**
A	469g	906g	860g		701g	609g	803g
B	457g	635g	769g		652g	694g	679g
C	629g	407g	728g		731g	450g	740g
D	596g	699g	755g		500g	585g	700g
E	388g	511g	609g		508g	616g	673g
F	543g	525g	732g		510g	723g	768g

3.2.2 Roller milling of mixed feeds

A 4765 g rock of quartzite was fed into the jaw crusher. The product obtained was split into four samples using the riffle splitter. One sample of 1159 g was used as a mixed feed to the roller mill using an 8 mm gap size.

The size analysis from sieving, of the feed, as well as the product (named experimental product particle size distribution), was represented, as illustrated in Table 3.4.

Table 3.4: Particle size distribution of the mixed feed.

Size class (mm)	Mass size class (g)
16.0 – 18.0	85
13.3- 16.0	62
11.2-13.3	161
8.0 -11.2	230
6.7- 8.0	63
0.0 - 6.7	583

To simulate the roller milling of the mixed feed, the data in Table 3.4 feed was multiplied by a breakage matrix (8mm gap size in this case), to obtain the product particle size distribution or simulated product particle size distribution. The experimental and the simulated product particle size distributions were then compared.

The same operation was duplicated for a mixed feed sample of 585 g using a 10 mm roller gap size.

Chapter 4: Results and Discussion

This chapter presents and discusses the analysis of the experimental data. It comprises two sections:

- Section 1 focuses on determining the breakage matrices for the three different gap sizes tested. The impact of the mass of the feed, the feed size and the gap size on the product size distribution and the breakage matrix is investigated.
- Section 2 considers fitting models to the elements of the breakage matrices. The milling ratio and the cumulative passing distribution are used as variables to estimate the breakage function. This fitted function is then used to predict the product distribution for any feed size distribution and gap size.

4.1 Breakage matrices

Tables 4.1a and 4.2a present the data for the retained product mass from the milling of feeds of different masses and different size classes (as defined in Table 3.3) for a gap size of 8 mm for Test 1 and Test 2, respectively. The ratios of the retained mass of product to the feed mass yields the breakage matrices. Table 4.1.b and Table 4.2.b give the breakage matrices for the 8 mm gap size for Tests 1 and 2, respectively. The data for the retained mass fractions and breakage matrices for gap sizes of 10 and 12 are given in Appendix A.

All the breakage matrices for Test 1, Test 2 and the three gap sizes were shown to be diagonal (Appendix B). This is justified by the fact that no agglomeration occurs and the product size is either equal to or smaller than the feed size (Gupta and Yan, 2006). This was similarly the case for Broadbent and Callcott (1956), who obtained diagonal breakage matrices from experimental cone crushing of coal. However, Campbell et al. (2001) obtained breakage matrices from roller milling of wheat grains that were not diagonal, i.e. not all elements above the diagonal were 0. This was due to the agglomeration of wheat grains (Campbell et al., 2001). Two factors occurred that caused the agglomeration. Firstly, the gap sizes were smaller than the feed size, which meant that all the feed wheat grains were crushed. Secondly, because of the physical properties of

wheat grain, compression sometimes occurs, when the wheat grains passed between the rollers, rather than breakage, which results in the particles becoming longer and thinner than the feed particles. Using sieve size as the method of size characterization, results in some of the product from roller milling of wheat grain to appear larger than the feed. This type of agglomeration does not typically occur in ores.

Table 4.1: Retained product mass and breakage matrix for Test 1 using an 8 mm gap size. (Size classes are defined as: A: 18-16mm; B: 16-13,3mm; C: 13,3-11,2mm; D:11,2-8mm; E:8-6,7mm.) Masses are reported in grams

(a) Retained product mass (reported in grams)

	A	**B**	**C**	**D**	**E**	**F**
Sieve (mm)	**469**	**457**	**629**	**596**	**388**	**543**
16	40.334	0	0	0	0	0
13.3	38.458	68.55	0	0	0	0
11.2	28.14	54.84	56.61	0	0	0
8	26.733	63.98	69.19	95.36	0	0
6.7	66.598	36.56	81.77	47.68	388	0
0	268.737	233.07	421.43	452.96	0	543

(b) Breakage matrix

Sieve size (mm)	**A**	**B**	**C**	**D**	**E**	**F**
16	0.086	0.000	0.000	0.000	0.000	0.000
13.3	0.082	0.150	0.000	0.000	0.000	0.000
11.2	0.060	0.120	0.090	0.000	0.000	0.000
8	0.057	0.140	0.110	0.160	0.000	0.000
6.7	0.142	0.080	0.130	0.080	1.000	0.000
0	0.573	0.510	0.670	0.760	0.000	1.000

Table 4.2: Retained product mass and breakage matrix for Test 2 using an 8 mm gap size.
(Size classes are defined as: A: 18-16mm; B: 16-13,3mm; C: 13,3-11,2mm; D:11,2-8mm; E:8-6,7mm.). Masses are reported in grams

(a) Retained product mass (reported in grams)

Sieve (mm)	A	B	C	D	E	F
	701g	**652g**	**731g**	**500g**	**508g**	**510g**
16	70.5	0	0	0	0	0
13.3	69	129	0	0	0	0
11.2	50.02	20	35	0	0	0
8	90	44	66	118	0	0
6.7	70	66	43	31	508	0
0	350	390	583	348	0	510

(b) Breakage matrix

Sieve (mm)	A	B	C	D	E	F
16	0.100	0.000	0.000	0.000	0.000	0.000
13.3	0.100	0.200	0.000	0.000	0.000	0.000
11.2	0.070	0.030	0.050	0.000	0.000	0.000
8	0.130	0.070	0.090	0.240	0.000	0.000
6.7	0.100	0.100	0.060	0.060	1.000	0.000
0	0.500	0.600	0.800	0.700	0.000	1.000

The elements of the diagonal of the breakage matrix represent the unbroken proportion of the feed. For illustration purposes: in Table 4.1.b, after feeding 469 g of size class A, 8.6% of the

original 465 g is unbroken; after feeding, 457 g of size class B, 15% of 457 g is unbroken. The ratio of 1 means that there is no breakage, and the size of the material remains unchanged. This occurs when the feed size is smaller than the gap size. It is apparent from Table 4.1.b and Table 4.2.b that a large proportion of material the remains unbroken, despite it apparently being larger than the gap size. For instance, considering size fraction A (16-18mm), 8.6% of this material remains unbroken for an 8 mm gap size for Test 1, while 10% is retained for Test 2. The same trend is also observed for size fraction B (13.3-16mm) with 15% (Test 1) and 20% (Test 2) remaining unbroken for an 8 mm gap size. While this was unexpected, the general shape of the jaw crusher product can help to explain this result.

The jaw crusher that was used to prepare feed to the roller mill has corrugated jaws and therefore produced some elongated particles. These particles are more likely to pass through the gap between the rollers than to pass through a sieve gap. Therefore, it is conceivable that elongated particles that would have been retained by a sieve, for instance in the 13.3-16mm range, may pass through the roller mill without being ground, depending on their contact orientation. As illustrated in Figure 4.1, the shape of jaw crusher product particles which are the feed to the roller mill, have three dimensions, namely: width; length; thickness. The contact made by a particle with the rolls can be in either of the dimensions. When the contact made by a particle has a dimension smaller than the roll gap, there is no breakage, while breakage may take place if the contact dimension that the particle presents is larger than the roll gap. The position of the particles in the mill is uncontrolled, but physically, the particles tend to land on the flat side after being dropped onto the surface of the rolls, which causes the thickness to be presented as the dimension of contact. In this orientation, the thickness may be less than the gap size and may not yield significant breakage or may yield no breakage at all.

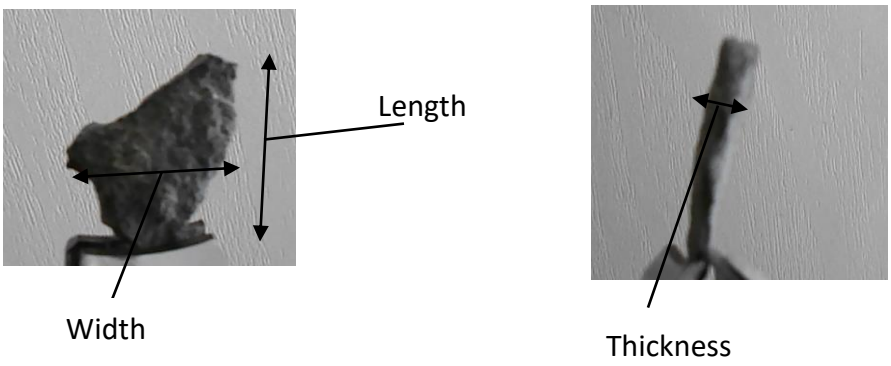

Figure 4.1: Dimensions of jaw crusher product particles.

Figure 4.2: 13,3 mm sieve size that retains particles that are thinner than the sieve size in one dimension

4.1.1 Impact of feed mass on the product size distribution

Experimental results from Test 1 and Test 2 were used to investigate the impact of feed mass on the product size distribution. Three cases are illustrated in Figure 4.3.

Appendix E gives the data for comparison between the following:

(1) PSD from the milling of size class A using 609 g for Test 2 and 906 g for Test 1 with a 10mm gap size.

(2) PSD from the milling of size class A using 803 g for Test 2 and 860 g for Test 1 with a 12mm gap size.

(3) PSD from the milling of size class B using 679 g for Test 2 and 769 g for Test 1 with a 12mm gap size.

(4) PSD from the milling of size class B using 652 g for Test 2 and 457 g for Test 1 with an 8mm gap size.

(5) PSD from the milling of size class C using 731 g for Test 2 and 629 for Test 1 with an 8mm gap size.

(6) PSD from the milling of size class C using 450 g for Test 2 and 407 g for Test 1 with a 10mm gap size.

It is clear that despite the variation in the feed mass, there is superposition of product size distributions from Test 1 and Test 2. That demonstrates: that the tests are reproducible; and that the feed mass does not strongly impact on the product size distribution. This was also observed by: Campbell et al. (2001) when roll milling wheat grains; Austin et al. (1980) in roll milling of coal. They assumed, as we do in this study, that particles break independently, which means there is no interaction between particles. However, when there is interaction between particles, as occurs in ball milling, the feed mass affects the product size distribution (Hlabangana et al., 2018).

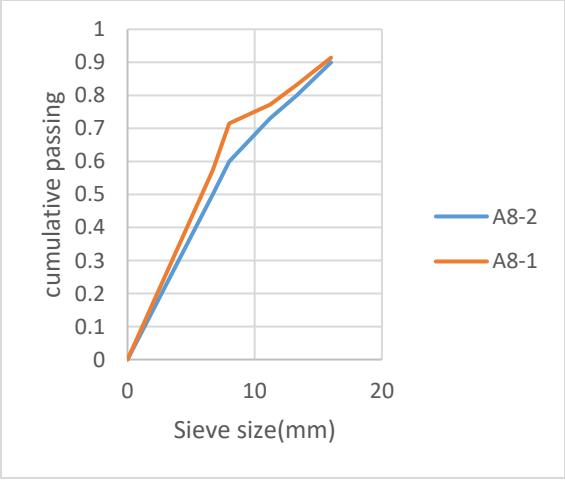

(a) Comparison of the product size distribution from the milling of 469 g (Test 1) and 701 g (Test 2) of size class A (16-18mm) with an 8 mm gap size.

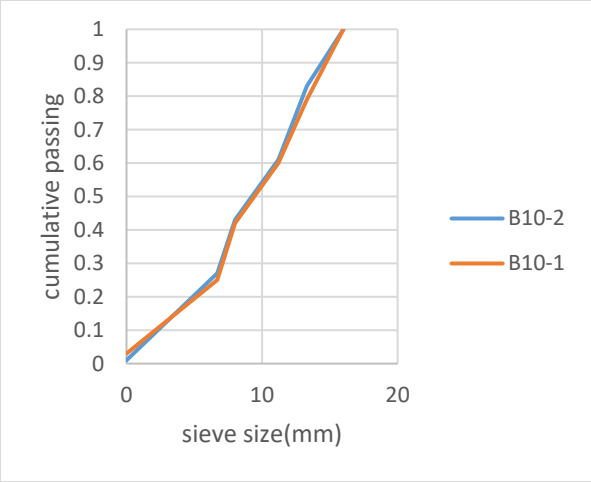

(b) Comparison of the product size distribution from the milling of 635 g (Test 1) and 694 g (Test 2) size class B (13.3-16mm) with a 10 mm gap size.

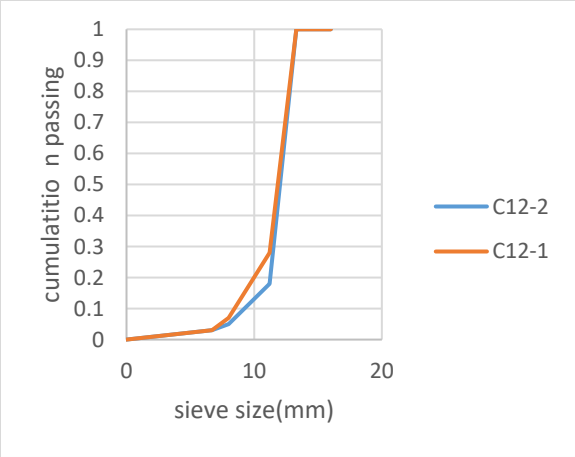

(c) Comparison of the product size distribution from the milling of 728 g (Test 1) and 740 g (Test 2) of size class C (11.2-13.3mm) with a 12 mm gap size.

Figure 4.3: Comparison of product size distribution (PSD) for Test 1 and Test 2.

4.1.2 Impact of feed size on the product size distribution

When investigating the impact of feed size on the PSD, the size classes D, E and F were not considered, as their breakage during roller milling was not significant.

Figure 4.4 shows the impact of feed size on product size distribution (PSD). As shown previously, the data from Tests 1 and 2 were very similar, therefore only the data from Test 2 is considered in the rest of this chapter. The data for the impact of feed size on product size distribution obtained from Test 1 are given in Appendix D.

It was demonstrated that the mass of product cumulatively passing a sieve size increases with decreasing feed size. For illustration purposes, in Figure 4.4a, it can be seen that 68%, 74% and 90% of the product from the milling of size classes A (16-18mm), B (13.3-16mm) and C (11.2-13.3mm) respectively pass through a 10 mm sieve. This shows that feed size affects product size distribution; therefore, it is considered to be a non-normalized breakage distribution and a non-normalized breakage function must be used to describe the distribution (Gupta and Yan, 2006).

This observation was also made by Campbell and Webb (2001) for roller milling of wheat grains. However, Austin et al. (1980) showed that the product size distributions from roller milling various feed sizes of coal could be superimposed; therefore, they could use a normalized breakage function (equation 2.10) to describe the milling. They used the procedure suggested by Austin et al. (1980) to model milling, where only fine particles (<400µm) in the product were considered for modeling; however, a deviation was observed for coarse particles (Campbell and Webb, 2001).

Austin et al. (1984) acknowledged that the assumption of normalization is used to reduce the number of breakage distribution parameters, because fewer parameters are needed to describe a normalized breakage function (see equation 2.10) than for a non-normalized breakage function. (See equation 2.11.) They also state that when coarse particles are considered in the product, the distribution becomes non-normalized.

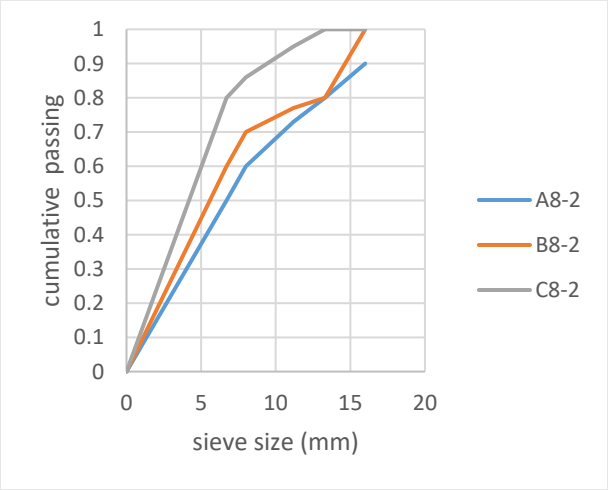

(a) PSD from the milling of feed materials in the size classes A (16-18mm), B (13.3-16mm) and C (11.2-13.3mm) using an 8mm gap size for Test 2.

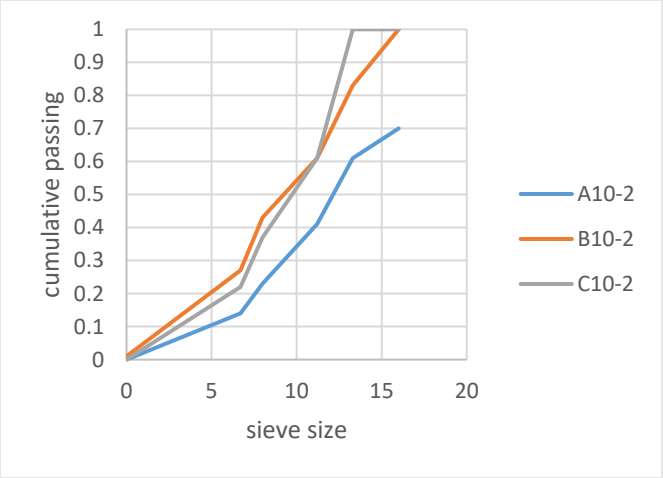

(b) PSD from the milling of feed materials in the size classes A (16-18mm), B (13.3-16mm) and C (11.2-13.3mm) using a 10 mm gap size for Test 2.

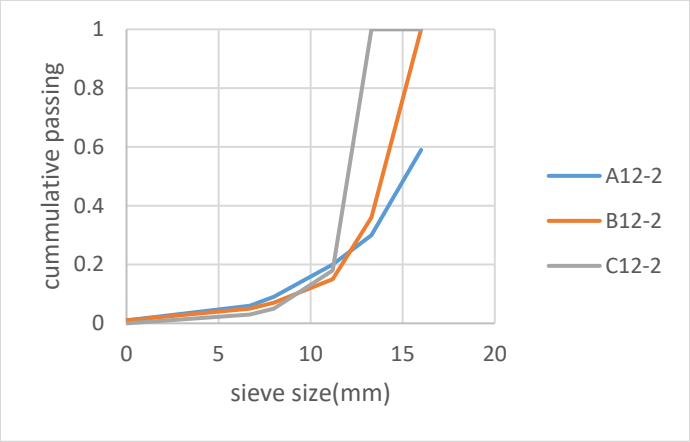

(c) PSD from the milling of feed materials in the size classes A (16-18mm), B (13.3-16mm) and C (11.2-13.3mm) using a 12 mm gap size for Test 2.

Figure 4.4: Comparison of the PSD from roller milling various feed sizes.

4.1.3 Prediction of the PSD using the breakage matrices and comparison of predicted PSD to experimentally measured PSD for a mixed feed

Broadbent and Callcott (1956) and Austin et al (1984) integrated the selection function in equation (2.6) to predict the PSD from cone milling and ball milling respectively. They acknowledged that the selection function, also called the probability of breakage or specific rate of breakage, depends on the residence time of particles in the mill.

However, for the roller milling of wheat grains, Campbell et al. (2001) state that the selection function is assumed to be unity since all the feed particles are milled. They also used equation (2.6) for prediction.

In this study, it is clear that the selection function is not unity since there is a significant percentage of unbroken particles. Nevertheless, as the residence time of particles cannot be controlled, the selection function in this case is believed to depend on the shape or dimension of particles when in contact with the rolls. Therefore, in this study the selection function is assumed to be embedded in the breakage matrix.

The next step to validate the approach used in this research was to mill feeds with a PSD (as opposed to feeds with a narrow PSD as was reported in Section 3.2 in the roller mill using

different gap sizes. We used equation (2.6) and the breakage matrices from Test 2 given in Appendix B to predict the PSD.

Equation (4.1) predicts the product of the roller mill for a feed of 1159 g with a feed PSD as described in Table 3.4 (Feed PSD in equation (4.1) , using an 8 mm gap size. The feed and product vectors in equation (4.1) represent the mass fractions retained on the sieves, and the breakage matrix for the 8mm gap size is given in Table 4.2.b. The vector Sim P.PSD represents the predicted PSD of the product while the vector Exp P.PSD in equation (4.1) represents the experimentally measured PSD.

Figure 4.5 and Figure 4.6 compare the experimental and predicted data using the breakage matrix for an 8 mm gap size (Table 4.2.b) and a 10 mm gap size (Appendix C.4) after feeding 1159 g and 585 g, respectively

Feed PSD (g) **8 mm breakage matrix** **Sim P.PSD (g)** **Exp P. PSD**

$$\begin{bmatrix} 58 \\ 62 \\ 161 \\ 230 \\ 63 \\ 583 \end{bmatrix} \times \begin{bmatrix} 0.1 & 0 & 0 & 0 & 0 & 0 \\ 0.1 & 0.2 & 0 & 0 & 0 & 0 \\ 0.07 & 0.03 & 0.05 & 0 & 0 & 0 \\ 0.13 & 0.07 & 0.09 & 0.24 & 0 & 0 \\ 0.1 & 0.1 & 0.06 & 0.06 & 1 & 0 \\ 0.5 & 0.6 & 0.8 & 0.7 & 0 & 1 \end{bmatrix} = \begin{bmatrix} 5.8 \\ 18.2 \\ 13.97 \\ 81.57 \\ 98.46 \\ 939 \end{bmatrix} \quad \begin{bmatrix} 0 \\ 8 \\ 43.4 \\ 93.7 \\ 113 \\ 898.6 \end{bmatrix} \quad \text{(Equation 4.1)}$$

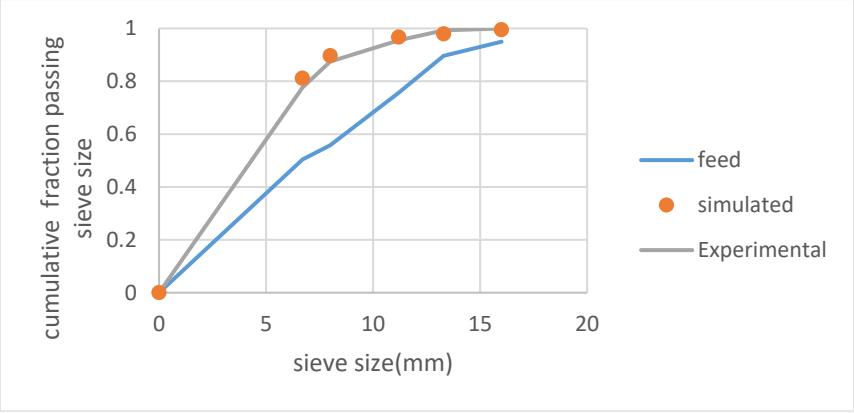

Figure 4.5: Comparison of experimental (Test2) and predicted data for roller milling a mixed feed (i.e.with PSD) using an 8 mm gap size

Feed PSD (g) **10 mm breakage matrix** **Sim P.PSD (g)** **Exp P. PSD**

$$\begin{bmatrix} 26 \\ 30 \\ 86 \\ 103 \\ 31 \\ 308 \end{bmatrix} \times \begin{bmatrix} 0.3 & 0 & 0 & 0 & 0 & 0 \\ 0.09 & 0.17 & 0 & 0 & 0 & 0 \\ 0.2 & 0.22 & 0.39 & 0 & 0 & 0 \\ 0.18 & 0.18 & 0.24 & 0.67 & 0 & 0 \\ 0.09 & 0.16 & 0.15 & 0.13 & 1 & 0 \\ 0.14 & 0.26 & 0.22 & 0.2 & 0 & 1 \end{bmatrix} = \begin{bmatrix} 7.8 \\ 7.44 \\ 45.34 \\ 99.73 \\ 64.43 \\ 358.96 \end{bmatrix} \quad \begin{bmatrix} 16.3 \\ 23.5 \\ 32.7 \\ 71.6 \\ 85.3 \\ 338.75 \end{bmatrix} \quad \text{(Equation 4.2)}$$

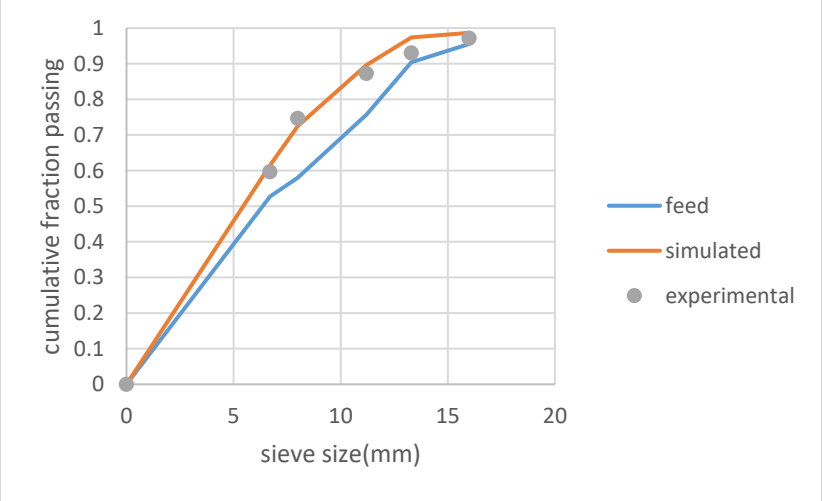

Figure 4.6: Comparison of predicted (Test 2) and experimental data for roller milling a mixed feed (i.e. with PSD) using a 10 mm gap size.

Figure 4.5 shows that when using an 8 mm gap size, 70% of the feed material passes through a 10 mm sieve size, while 90% of the product passes through a 10 mm sieve size. It also shows that the 5 mm sieve size allows 40% of the feed and 60% of the product to pass. It is then clear that, for a given feed material, the cumulative passing of a sieve size increases after breakage.

Figure 4.5 and Figure 4.6 compare the experimental data and the predicted data. The similarity of the experimental data and predicted data indicates that equation (2.5) can be used to predict the breakage of roller milling of quartzite.

4.2 Correlating the elements of the breakage matrix to the milling ratio and feed size

4.2.1 Correlation between the breakage function and milling ratio

The mathematical function that describes the product size distribution of a material from the breakage of a single particle or a narrow size, is called a breakage distribution function or breakage function (Kelly and Spottiswood, 1990). The breakage function has been shown to depend on the milling ratio (ratio of roll gap size to feed size) (Campbell et al., 2001).

Table 4.3 illustrates the values of the milling ratio used in the experiments in this work. The arithmetic mean of the lower and upper sieve size was used to represent each feed size class, giving values as follows: A (16-18mm) = 17 mm; B (13.3-16mm) = 14.65 mm; C (11.2-13.3mm) = 12.25 mm.

Table 4.3: Values of milling ratio used in this work.
(The milling ratio is the ratio of roll gap size (in mm) to the average value of the feed size class (in mm).

Roller gap	A:17	B:14.65	C:12.25
8	0.471	0.546	0.653
10	0.588	0.683	0.816
12	0.706	0.819	0.980

Table 4.4 gives the product cumulative passing versus the milling ratio for Test 2 for the 8, 10 and 12 mm gap sizes. (Also see Appendix F.) As indicated in Table 4.4.a, the cumulative passing of value 0.9 for an 8 mm gap size, means that 90% of the material in the product passes the sieve with a mean size of 17mm, when using an 8/17 milling ratio. A value of 1 means that no breakage occurred and all the feed material passed through that sieve size. It was noticed that the sieve sizes (mean size) of 17 and 14.65 mm did not provide sufficient information about breakage over all three milling ratios, as elements of these were 1. Furthermore, there was no information for the 3,35 mm size, as no (or very little) material reported to this size class. Therefore, only the information from sieve sizes 12.25, 9 and 7.35 mm was used to correlate the breakage function

with the milling ratio. Essentially, the elements matrix in Table 4.4 are the sum of the elements of the breakage matrix in equation (4.1) for all sizes smaller than that sieve size.

Table 4.4: Cumulative passing versus milling ratio for different gap sizes based on Test2
(a) Cumulative passing versus milling ratio for an 8mm gap size:

Sieve (mm)	8/17	8/14.65	8/12.25
17	0.9	1	1
14.65	0.8	0.8	1
12.25	0.73	0.77	0.95
9.6	0.6	0.7	0.86
7.35	0.5	0.6	0.8
3.35	0	0	0

(b) Cumulative passing versus milling ratio for a 10 mm gap size.

Sieve (mm)	10/17	10/14.65	10/12.25
17	0.7	1	1
14.65	0.61	0.83	1
12.25	0.41	0.61	0.61
9.6	0.23	0.43	0.37
7.35	0.14	0.27	0.22
3.35	0	0.01	0

(c) Cumulative passing versus milling ratio for a 12 mm gap size.

	12/17	**12/14.65**	**12/12.25**
17	0.59	1	1
14.65	0.3	0.36	1
12.25	0.2	0.15	0.18
9.6	0.09	0.07	0.05
7.35	0.06	0.05	0.03
3.35	0.01	0.01	0

The data in Table 4.4 was plotted in Figure 4.7 and it was seen that a log-normal function (equation 4.3) fits the product size distribution for all the feed sizes, as illustrated in Figure 4.7.

$$B(x_i; x_j) = \alpha ln\left(\frac{G}{x_j}\right) + \beta \qquad \text{(Equation 4.3)}$$

Where: $B(x_i; x_j)$ is the cumulative passing sieve of size x_i from the milling of a feed size class of size x_j;

α and β are fitted coefficients;

G is the gap size.

In this model, the values of x_i were limited to values of 12.25, 9.6, and 7.35mm, as these were the only product sieve sizes considered. The feed size classes of x_j, were: 17 (called fraction A); 14.65 (called fraction B); and 12.25mm (called fraction C). α and β are the coefficients that are determined from the best fit of the model to the experimental data. These coefficients were found to be polynomial functions of second degree of feed size, as illustrated in Figure 4.8.

Figure 4.7.a shows a plot of the experimental data and the best fit log normal distribution for the cumulative mass of the product passing through the 12.25 mm sieve versus the milling ratio for the three different feed size fractions. The blue line represents the best log normal fit of the cumulative mass of the product passing the 12.25 mm sieve size versus the milling ratio for feed

fraction A. The upper point of the fit indicates the cumulative mass of the product passing through the 12.25 mm sieve size for a milling ratio of 8/17 taken from Table 4.4a. The middle point of the model represents the cumulative mass of the product passing through the 12.25 mm sieve size for a 10/17 milling ratio, taken from Table 4.4.b. The lower point of the model indicates the cumulative mass of the product passing through the 12.25 mm sieve size using a 12/17 milling ratio, as illustrated in Table 4.4.c.

The model given in equation (4.2) was used to fit the measured product size distribution. For feed fraction A and sieve size 12.25, the best fit for this equation is given by:

$$y = -1.312\ \ln(x) - 0.2673 \qquad \text{(Equation 4.4)}$$

Where: $y = B(x_i; x_j)$ the cumulative passing $x_i = 12.25$ mm from the milling of size class $x_j = A$;

$\alpha = -1.312$;

$\beta = -0.2673$;

$x = \frac{G}{A}$;

A =17 as mean size.

The "goodness of fit", R-squared for size class A, gives 0.9963, which means that 99.63% of the data fit the model (Walkenbach, 2007).

It was found that the "goodness of fit" was satisfactory in general, and the same function of log-normal fits the milling of all the feed sizes.

Figures 4.7.b and 4.7.c illustrate the log normal fit of the breakage function for the 9.6 mm and 7.35 mm sieve sizes, respectively. It was similarly found that the "goodness of fit" for these was satisfactory in general, with the lowest R^2 being 0.8947.

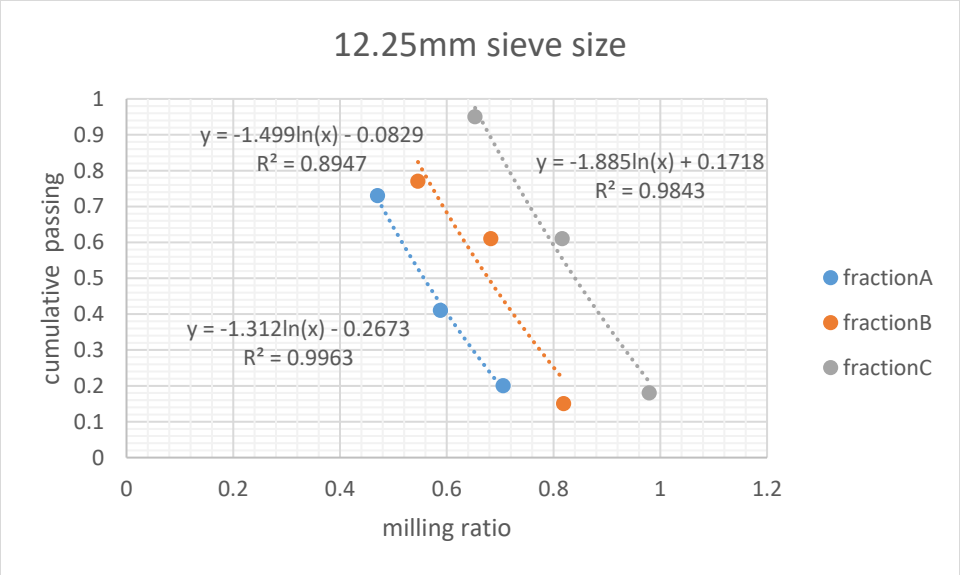

(a) Cumulative mass of product passing through the 12.25 mm sieve size versus the milling ratio for feed sizes 17 mm (fraction A), 14.65 mm (fraction B) and 12.25 mm (fraction C).

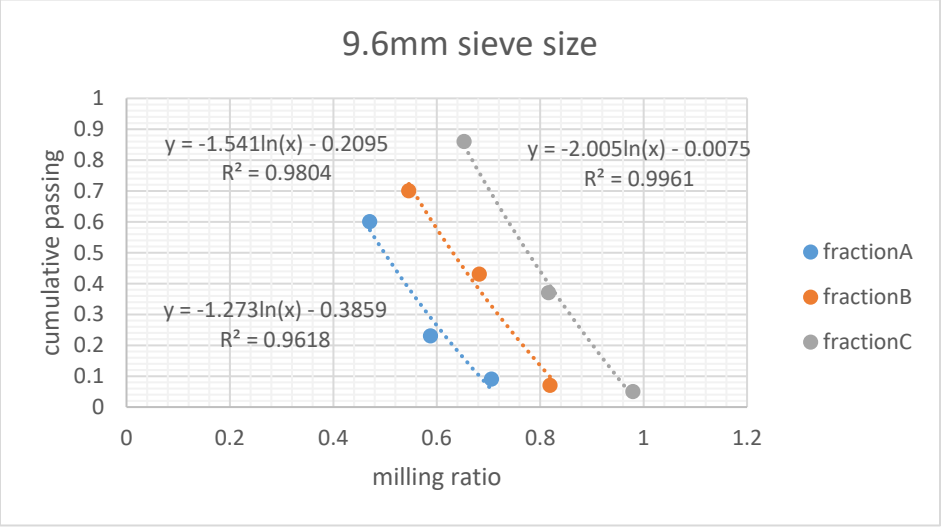

(b) Cumulative mass of product passing through the 9.6 mm sieve size versus the milling ratio for feed sizes 17 mm (fraction A), 14.65 mm (fraction B) and 12.25 mm (fraction C).

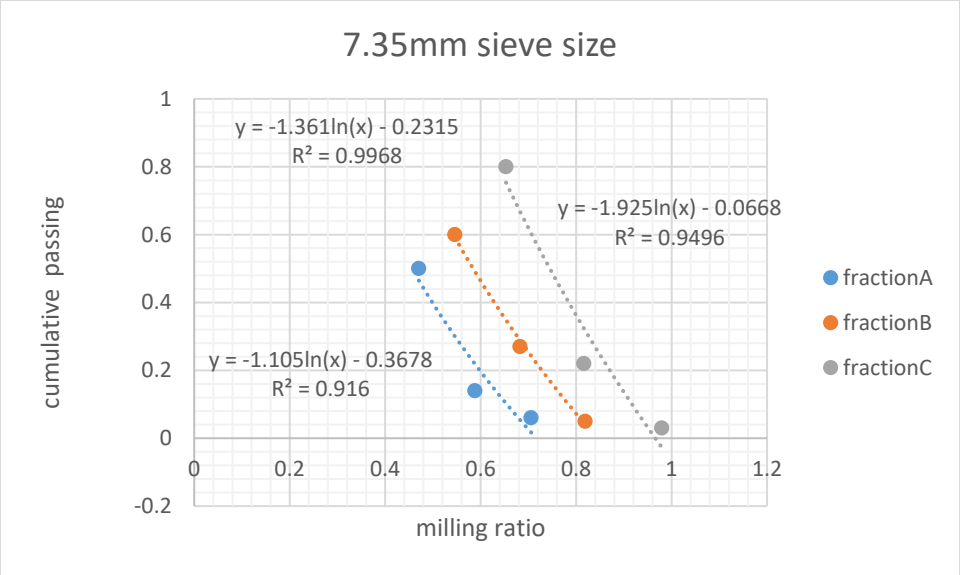

(c) Cumulative mass of product passing through the 7.35 mm sieve size versus the milling ratio for feed sizes 17 mm (fraction A), 14.65 mm (fraction B) and 12.25 mm (fraction C).

Figure 4.7: Cumulative mass of product passing through sieve sizes versus the milling ratio.

4.2.2 Correlating the fitted $\boldsymbol{\alpha}$ and $\boldsymbol{\beta}$ parameters to feed size

Figure 4.7 demonstrates that although the same log normal function describes the cumulative passing for all the feed sizes (A, B and C), there is no superposition of the cumulative size distribution graphs. This indicates that the breakage distribution is non-normalizable and, therefore, each trend-line is characterized by specific values of the coefficients α and β.

The correlation used by Campbell et al. (2001) for roller milling of wheat grains was used in this research on quartzite. Campbell et al. (2001) fitted quadrative equations to describe the variation of the parameters α and β with the feed size x_j, for a given product size x_i:

$$\alpha(x_i) = a_\alpha + b_\alpha x_j + c_\alpha x_j^2$$

$$\beta(x_i) = a_\beta + b_\beta x_j + c_\beta x_j^2$$

Table 4.5 summarizes the values of α and β (from Figure 4.8) for each feed size x_j. The analysis of the data (from Table 4.5) was done using Microsoft Excel, by plotting α and β versus the feed size x_j and fitting a quadratic equation to the data (equation 4.5 and 4.6). For example, equation (4.5)

and equation (4.6) describe the variation of α and β for a product size (x_i) of 12.25mm for the data shown in Figure 4.8a. The blue line (equation 4.5) refers to the variation of α and the orange line (equation 4.6) refers to the variation of β.

$$\alpha(x_i = 12.25) = -0.0171x_j^2 + 0.621x_j - 6.9253 \quad \text{(Equation 4.5)}$$

$$\beta(x_i = 12.25) = 0.0058x_j^2 - 0.2628x_j + 2.5168 \quad \text{(Equation 4.6)}$$

Figure 4.8b and Figure 4.8c illustrate the variation of α and β using a 9.6mm and 7.35 mm sieve size, respectively.

Table 4.5: Variation of α and β with product size x_i (indicated by sieve size) and feed size x_j.
(Indicated by: A = 17 mm; B = 14.65 mm; C = 12.25mm.)

(a) 12.25 mm sieve size

	A	**B**	**C**
	17	**14.65**	**12.25**
α	-1.312	-1.499	-1.885
β	-0.2673	-0.0829	0.1718

(b) 9.6 mm sieve size

α	-1.2746	-1.54214	-2.00574
β	-0.3903	-0.21272	-0.00971

(c) 7.35 mm sieve size

α	-1.0938	-1.35271	-1.91923
β	-0.3785	-0.23945	-0.07236

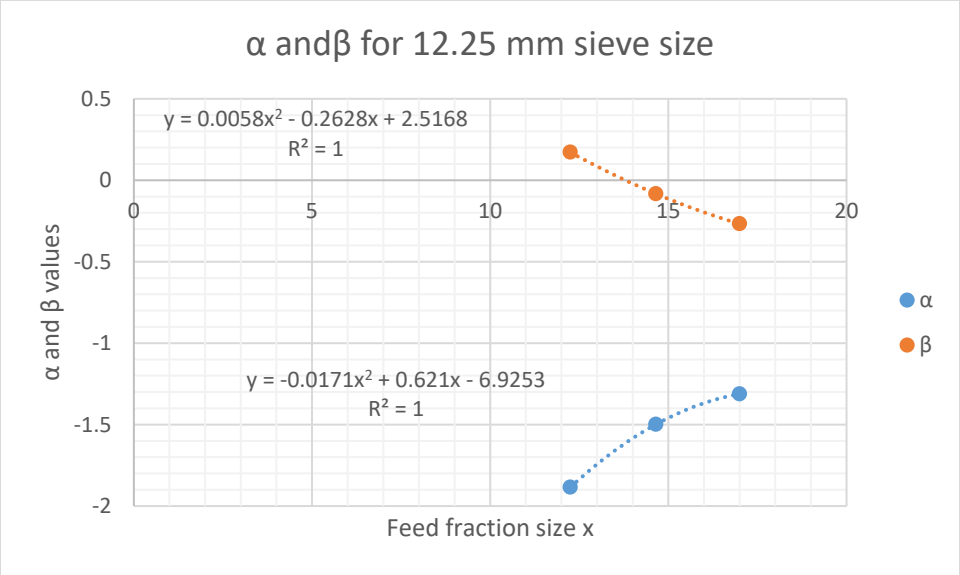

(a) Variation in α and β for product size x_i = 12.25 mm (sieve size) for different feed sizes.

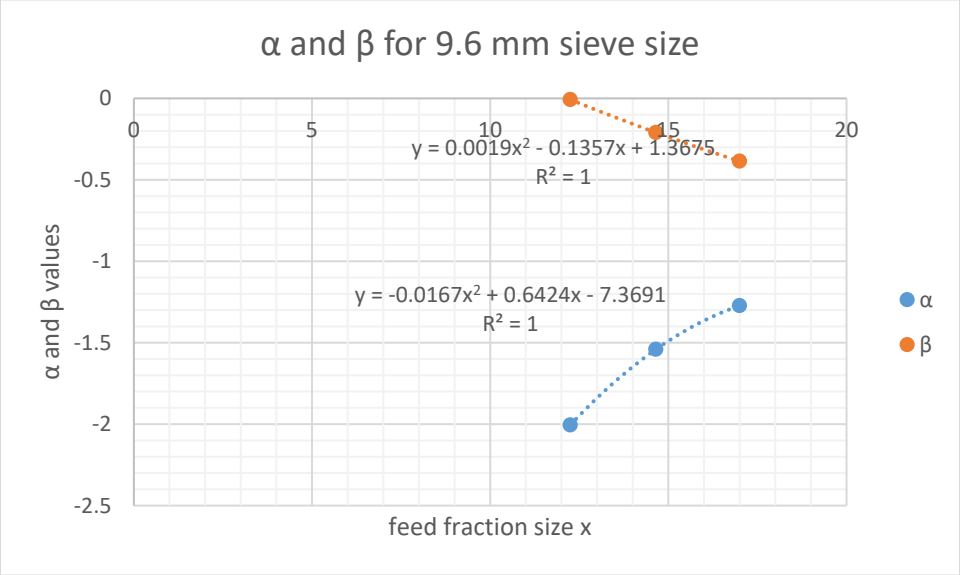

(b) Variation in α and β variations for product size x_i = 9.6 mm (sieve size) for different feed sizes.

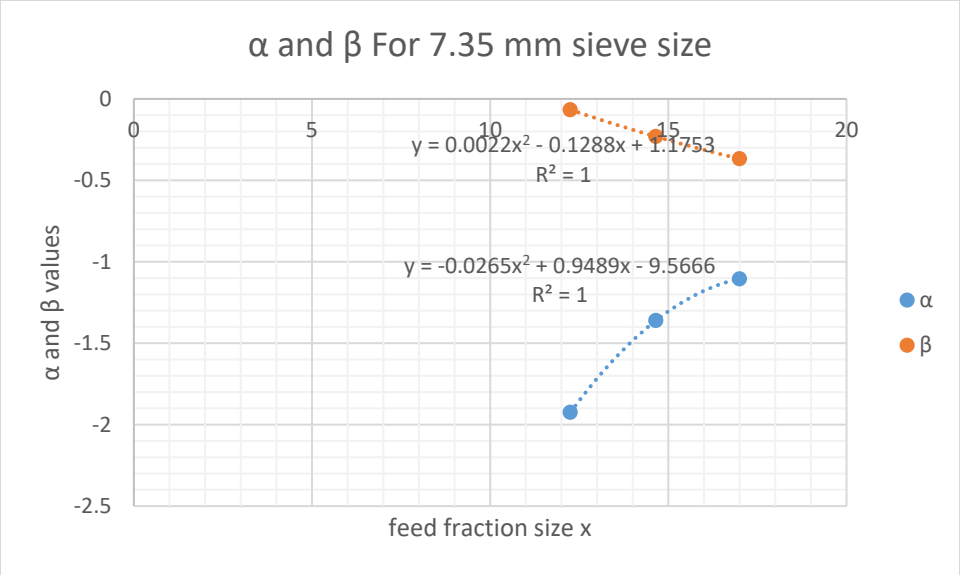

(c) Variation in α and β for product size x_i = 7.35 mm sieve size (sieve size) for different feed sizes.

Figure 4.8: Variation in α and β with feed size x_j.

((a) α and β variations for 12.25 mm sieve size (b) α and β variations for 9.6 mm sieve size (c) α and β variations for 7.35 mm sieve size.)

4.2.3 Using the fitted model to predict the PSD

In order to predict the PSD, the following steps are:

(1) Specify the sieve (product size x_j) size of interest.

(2) Use the appropriate α and β correlation from Table 4.5.

(3) Use equation (4.3) to calculate B (x_i,x_j) for a given milling ratio.

(4) Having calculated all the B (x_i,x_j), calculate the cumulative passing for a given feed PSD.

For illustration purposes, the prediction for a x_j = 12.25m (i.e. sieve size) for a 20 mm feed size gave the following results:

α = -1.3033 and β = -0.4192, using equation (4.5) and equation (4.6), respectively.

The values of milling ratio 8/20, 10/20 and 12/20 were used along with α and β values in the equation (4.3), in order to determine the cumulative passing 12.25 mm sieve size. These results

are illustrated by the yellow curve in Figure 4.9a. Similarly, the dark-blue curve is the prediction for milling a 13mm feed size.

The comparison between the experimental data (denoted A, B and C in Figure 4.9a) and the model (yellow and dark-blue curves) for 20mm and 13mm feed sizes, respectively, show that the model is acceptable. It can be seen in Figure 4.9.a that the predicted cumulative mass passing for 12.25 mm sieve size from the milling of 20 mm feed size is just below the experimentally measured curved for a feed A (17mm). Similarly, the predicted product size distribution from the milling of a 13 mm feed size lies between the experimentally measured feed sizes of B and C, as expected. The same trend was also observed for the prediction using a 9.6 mm sieve size, as shown in Figure 4.9.b.

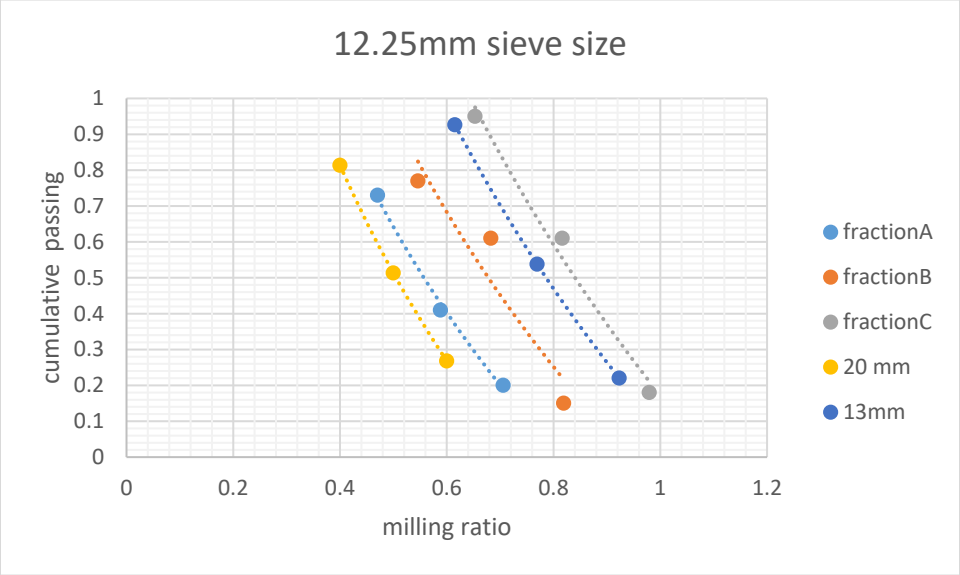

(a) Comparison of the model predictions for the cumulative mass passing through a 12.25 mm sieve size for a 20 mm and 13 mm feed size to the experimental data for feeds sizes: 17 mm (fraction A); 14.65 mm (fraction B); 12.25 mm (fraction C).

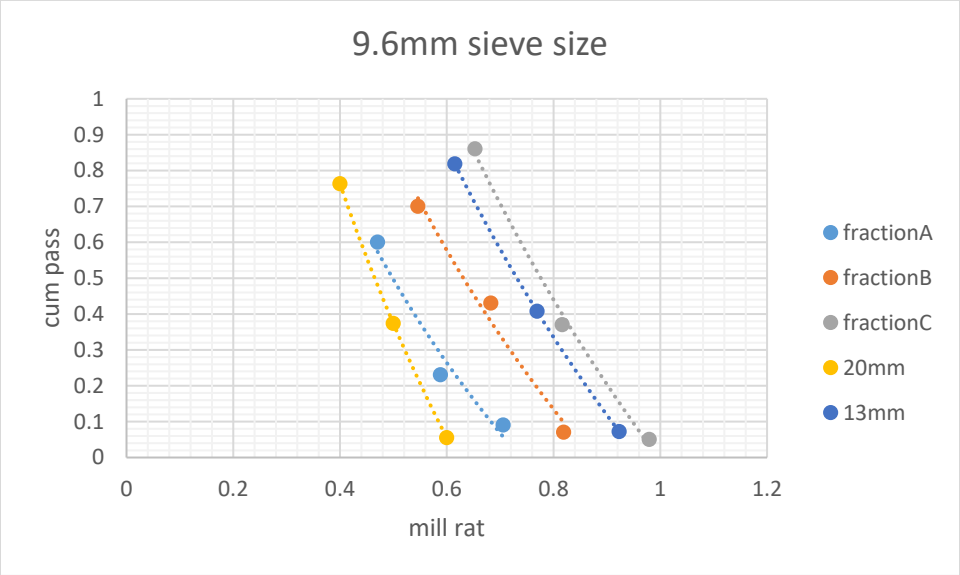

(b) Comparison of the model predictions for the cumulative mass passing through a 9.6 mm sieve size for a 20 mm and 13 mm feed size to the experimental data for feeds sizes: 17 mm (fraction A); 14.65 mm (fraction B); 12.25 mm (fraction C).

Figure 4.9: Comparison of the prediction cumulative mass passing to the experimental data.

Unfortunately, we could not validate the predictions experimentally, as we could not prepare material of 20mm and 13mm, as the test jaw crusher used for preparing the feed size fractions was not flexible.

Chapter 5: Conclusion

A quartzite feed was split into three narrow size classes and each of these feeds was milled in a roller mill using three different gap sizes. The experimental data was used to determine the breakage matrix for each gap size. The breakage matrices were found to be diagonal, as the product size was either equal to or smaller than the feed size. The superposition of the experimental and predicted results, using the breakage matrix equation, proved that the selection function can be incorporated into the breakage matrix for modelling the roller milling of quartzite.

It was shown that the mass of feed milled does not impact the product PSD, as the particles break independently of each other in the roller mill. However, the feed size was found to affect product PSD. This confirmed that the breakage distribution of quartzite with roller milling is not normalized.

Using the milling ratio and cumulative passing as variables, the product PSD for roller milling of quartzite was found to follow a log-normal distribution that depended on the milling ratio. This distribution could be described by two coefficients, namely α and β. It was shown that α and β for a given product size could be correlated to the feed size using a quadratic form.

The coefficients of the quadratic function were considered constants for a given product size, and this allowed the prediction of the cumulative passing of the product for different feed sizes. The comparisons between the model predictions and the experimental data supports the approach used to estimate the breakage function for roller milling of quartzite.

Further research is necessary to validate experimentally the simulated prediction of the 20 mm and 13 mm feed size. To achieve this, the use of a flexible jaw crusher with similar specifications is recommended.

It is also important to determine if the coefficients of the quadratic equation for the specific sieve sizes of 7, 35; 9, 6; and 12, 25 mm are constants, so that they can be considered as breakage parameters for roller milling of quartzite.

The approach used in this research shows that the behavior of a roller mill can be simply modeled, and this might be useful for the modeling and optimization of industrial roller mills.

References

1) ASCE. (2008). *Standard guideline for fitting saturated hydraulic conductivity using probability density function (ASCE/EWRI 50-08); standard guideline for calculating the effective saturated hydraulic conductivity (ASCE/EWRI 51-08)*. Reston, VA: American Society of Civil Engineers, pp.1-28. [Accessed 15 June 2019].
2) Atherton, K. (2017). *Excavator*. [image] Available at: https://www.popsci.com/bagger-288-facts/ [Accessed 21 May 2019].
3) AUBEMA. (2014). *Single roll crusher*. [image] Available at: http://www.tlt.as /Undersider /documents/RollCrusher1Single.pdf [Accessed 5 May 2019].
4) Austin, L., and Bhatia, V., (1971/7). Experimental methods for grinding studies in laboratory mills. Powder Technol. 5, 261-266.
5) Austin, L., Klimpel, R. and Luckie, P. (1984). *Process engineering of size reduction*. New York: Soc. of Mining Engineers, pp.181-194.
6) Austin, L. and Luckie, P. (1972). The estimation of non-normalized breakage distribution parameters from batch grinding tests. *Powder Technology*, 5(5), pp.267-271.
7) Austin, L., Van Orden, D., McWilliams, B., Perez, J. and Shoji, K. (1981). Breakage parameters of some materials in smooth roll crushers. *Powder Technology*, 28(2), pp.245-251.
8) Austin, L., Van Orden, D. and Pérez, J. (1980). A preliminary analysis of smooth roll crushers. *International Journal of Mineral Processing*, 6(4), pp.321-336.
9) Aydinap, C. (2012). *An Introduction to Mineralogy*. Rijeka, Croatia: In Tech, pp.3-11.
10) Barrios, G. and Tavares, L., 2021. A preliminary model of high pressure roll grinding using the discrete element method and multi-body dynamics coupling. *International Journal of Mineral Processing*, p.2.

11) Broadbent, S. and Callcott, T. (1956). A matrix analysis of processes involving particle assemblies. *Philosophical Transactions of the Royal Society A: Mathematical, Physical and Engineering Sciences*, 249(960), pp.99-123.

12) BRUKER. (2019). *X-Ray Fluorescence Spectrometer*. [image] Available at: https://www.bruker.com/products/x-ray-diffraction-and-elemental-analysis/handheld-xrf/x-ray-fluorescence-spectrometer.html [Accessed 7 August 2019].

13) Cabello, M., Peres, A., Martins, A. and Pereira, C. (2013). Use of quartzite quarries wastes in civil construction. *Key Engineering Materials*, 548, pp.135-140.

14) Campbell, G. and Webb, C. (2001). On predicting roller milling performance. Part I: the breakage equation. *Powder Technology*, 115(3), pp.234-242.

15) Campbell, G., Webb, C., Bunn, P. and Hook, S. (2001). On predicting roller milling performance. Part II: The breakage function. *Powder Technology*, 115(3), pp.243-255.

16) Chibundo Princewill, N., 2017. Development and Performance Evaluation of Improved Hammer Mill. *Scientific and Engineering Research*, 4(8), p.160.

17) Cotabarren, I., Schulz, P., Bucalá, V. and Piña, J (2008). Modeling of an industrial double-roll crusher of a urea granulation circuit. *Powder Technology*, 183(2), pp.224-230.

18) Das, P. (2001). Use of cumulative size distribution to back-calculate the breakage parameters in batch grinding. *Computers & Chemical Engineering*, 25(9-10), pp.1235-1239.

19) Deniz, V. (2011). Effects of two important parameters on capacity of a laboratory Jaw Crusher of different coals: Choke feed level and effective reduction ration. *International Journal of Coal Preparation and Utilization*, 31(6), pp.335-345.

20) Edmiston, G. (2019). *Factors to Consider When Selecting the Proper Roll Crusher for an application* [online] McLanahan. Available at: https://www.mclanahan.com/blog/ factors-to-consider-when-selecting-the-proper-roll-crusher-for-an-application [Accessed 14 December 2019].

21) Elzea Koge, J., Trivedi, N., Barker, J. and Krukowski, S., 2006. *Industrial Minerals & Rocks: Commodities, Markets, and Uses*. 7th ed. Colorado, USA: society for Mining, Metalurgy, and Exploration, Inc, p.843.

22) Fistes, A., Rakić, D., Takači, A. and Brdar, M. (2013). Using the breakage matrix approach to define the optimal particle size distribution of the input material in a milling operation. *Chemical Engineering Science*, 102, pp.346-353.

23) Fuerstenau, M. and Han, K. (2009). *Principles of Mineral Processing*. Littleton, Colo.: Society for Mining, Metallurgy, and Exploration, pp.79-90.

24) Fuerstenau, M. and Han, K. (2009). *Principles of Mineral Processing*. [ebook] Colorado, USA: Society for Mining, Metallurgy, and Exploration, pp.80-82.

25) Garba, N., Yamusa, Y., Isma'ila, A., Habiba, S., Garba, Z., Musa, Y. and Kasim, S. (2013). Heavy metal concentration in soil of some mechanic workshops of Zaria-Nigeria. *International Journal of Physical Sciences*, 8(44), pp.2029-2034.

26) Gay, S. (2004). A liberation model for comminution based on probability theory. *Minerals Engineering*, 17(4), pp.525-534.

27) Ghandi, S. and Sarkar, B. (2016). Essentials of minerals exploration and evaluation. *Elsevier*, [online] pp.235-255.

28) Gupta, A. and Yan, D.S. (2006). *Introduction to Mineral Processing Design and Operation*. Perth, Australia: Elsevier Science, pp.99-128.

29) Hameed Karim, H. (2012). Using quartzite rocks for manufacturing refractory silica bricks. *Special Issue of Engineering and Development Journal*, pp.1-21.

30) Haque E (1991). Application of size reduction theory to roller mill design and operation. *Cereal Food World* 36:368–374

31) Hlabangana, N., Danha, G. and Muzenda, E. (2018). Effect of ball and feed particle size distribution on the milling efficiency of a ball mill: An attainable region approach. *South African Journal of Chemical Engineering*, 25, pp.79-84.

32) Hussein H, K., Hisham K, A. and Oday A, A., 2017. Using Quartzite Rocks For Manufacturing Refractory Silica Bricks To Resist Concentrated Acids. *Special Issue of Engineering and Development Journal*, pp.1073-1092.

33) Ipek, H. and Goktepe, F. (2011). Determination of grindability characteristics of zeolite. *Physicochemical Problems of Mineral Processing*, 47, pp.183-192.

34) Jankovic, A., Ozer, C., Valery, W. and Duffy, K., 2016. Evaluation of HPGR and VRM for dry comminution of mineral ores. *Journal of Mining and Metallurgy A: Mining*, 52(1), pp.11-25.

35) Junior, I., Ribeiro, R., da Silva, M., Aureliano, F., Costa, A. and Garcia, V., 2019. Study of reactive powder concrete using quartzite tailings from the state of Minas Gerais - Brazil. *Procedia Manufacturing*, 38, pp.1758-1765.

36) Kelly, E. and Spottiswood, D. (1982). *introduction to mineral processing*. [ebook] New York: John Wiley & Sons, pp.130-158.

37) Kelly, E. and Spottiswood, D. (1990). The breakage function: What is it really? *Minerals Engineering*, 3(5), pp.405-414.

38) King, H. (2005). *A Specimen of Quartzite*. [image] Available at: <https://geology.com/rocks/quartzite.shtml> [Accessed 29 June 2020].

39) Klimpel, R. and Austin, L. (1965). the statistical theory of primary breakage distributions for brittle materials. *Transactions of the Society of Mining Engineers*, 232(88).

40) Klimpel, R. and Austin, L. (1977). The back-calculation of specific rates of breakage and non-normalized breakage distribution parameters from batch grinding data. *International Journal of Mineral Processing*, 4(1), pp.7-32.

41) Lynch, R. and Morrison, A. (1999). Simulation in mineral processing history: Present status and possibilities. *Journal of the Southern African Institute of Mining and Metallurgy*, [online] 99(6), pp.283 - 288.

42) Mining for Zambia. (2016). *Blasting*. [image] Available at: https://miningforzambia.com/ five-things-didnt-know-blasting/ [Accessed 13 July 2019].

43) Mosher, J. (2016). Comminution circuits for gold ore processing. *Gold Ore Processing*, pp.259-277.

44) Perrone, A. and Finlayson, J. (2014). Application of portable X-ray fluorescence (XRF) for sorting commingled human remains. *Methods in Recovery, Analysis, and Identification*, pp.145-165.

45) Petrakis, E. and Komnitsas, K. (2017). Improved modeling of the grinding process through the combined use of matrix and population balance models. *Minerals*, 7(5), p.67.

46) Pryor, E. (1965). *Mineral Processing*. 3rd ed. [ebook] London: Elsevier Applied Science, pp.31-70.

47) Reichert, M., Gerold, C., Fredriksson, A., Adolfsson, G. and Lieberwirth, H. (2014). Research of iron ore grinding in a vertical roller-mill.

48) Reid, K. (1965). "A Solution to the Batch Grinding Equations," *Chem. Eng. Set*, Vol. 20, p. 953

49) Rogers, R. and Shoji, K. (1983). A double-roll crusher model applied to a full scale crusher. *Powder Technology*, 35(1), pp.123-129

50) Rozenbaum, O., Machault, J., Le Trong, E., George, Y., Tankeu, N. and Barbanson, L. (2016). Ore fragmentation modelling for the evaluation of the liberation mesh size. *HAL*, [online] pp.1447-1450.

51) Rudnick, R. and Fountain, D., 1995. Nature and composition of the continental crust: A lower crustal perspective. *Reviews of Geophysics*, 33(3), p.267.

52) Saravacos, G. and Kostaropoulos, A. (1928). *Food Engineering Series*. New York: Kluwer Academic/Plenum, pp.150-155.

53) Singh, R., Sarbajna, C., Basu, H. and Venkateshwarlu, M. (2017). Geochemical characterization of quartzites of the Srisailam Banganapalle and Paniam formations from the northern part of the Cuddapah Basin, Telangana and Andhra Paradesh. *Applied Geochemistry*, 19(1), pp.34-43.

54) Swain, A., Patra, H. and Roy, G. (2011). *Mechanical Operations*. 1st ed. New Delhi, India: Mc Graw-Hill, pp.57-89.

55) Walkenbach, J. (2007). *Excel 2007 Charts*. Indianapolis, In: Wiley Pub., Inc., pp.150-170.

56) Wang, J., Chen, Q., Kuang, Y., Lynch, A. and Zhuo, J. (2009). Grinding process within vertical roller mills: experiment and simulation. *Mining Science and Technology (China)*, 19(1), pp.97-101.

57) Weichert, R., 1988. Correlation between probability of breakage and fragment size distribution of mineral particles. *International Journal of Mineral Processing*, 22(1-4), pp.1-8.

58) Whiten, W. (1974). A matrix theory of comminution machines. *Chemical Engineering Science*, 29(2), pp.589-599.

59) Wills, B. (1985). *Mineral Processing Technology*. 3rd ed. Cornwall, England: Pergamon Press, pp.133-175.

60) Wilson, J. (2010). *Minerals and Rocks*. [ebook] Richard & Ventus Publishing Aps, pp.10-45.

Appendix A: Product mass retained

A.1: Product mass retained from the milling of feed masses for Test 1.

A.1.1: Product mass retained using an 8 mm gap size for Test 1.

	A	B	C	D	E	F
Sieve (mm)	**469**	**457**	**629**	**596**	**388**	**543**
16	40.334	0	0	0	0	0
13.3	38.458	68.55	0	0	0	0
11.2	28.14	54.84	56.61	0	0	0
8	26.733	63.98	69.19	95.36	0	0
6.7	66.598	36.56	81.77	47.68	388	0
0	268.737	233.07	421.43	452.96	0	543

A.1.2: Product mass retained using a 10 mm gap size for Test 1.

	A	B	C	D	E	F
Sieve (mm)	**906**	**635**	**407**	**699**	**511**	**525**
16	226.5	0	0	0	0	0
13.3	117.78	133.35	0	0	0	0
11.2	280.86	120.65	175.01	0	0	0
8	181.2	114.3	77.33	489.3	0	0
6.7	99.66	107.95	89.54	139.8	511	0
0	144.96	139.7	65.12	69.9	0	525

A.1.3: Product mass retained using a 12 mm gap size for Test 1.

	A	B	C	D	E	F
Sieve (mm)	**860**	**769**	**728**	**755**	**609**	**732**
16	301	0	0	0	0	0
13.3	180.6	438.33	0	0	0	0
11.2	120.4	130.73	524.16	0	0	0
8	111.8	92.28	152.88	755	0	0
6.7	51.6	38.45	29.12	0	609	0
0	94.6	69.21	21.84	0	0	732

A.2: Product mass retained from the milling of feed masses for Test 2:

A.2.1: Product mass retained using an 8 mm gap size.

Sieve (mm)	**A**	**B**	**C**	**D**	**E**	**F**
	701 g	**652 g**	**731 g**	**500 g**	**508 g**	**510 g**
16	70.5	0	0	0	0	0
13.3	69	129	0	0	0	0
11.2	50.02	20	35	0	0	0
8	90	44	66	118	0	0
6.7	70	66	43	31	508	0
0	350	390	583	348	0	510

A.2.2: Product mass retained using a 10 mm gap size.

Sieve (mm)	A	B	C	D	E	F
	609 g	**694 g**	**450 g**	**585 g**	**616 g**	**723 g**
16	182.2	0	0	0	0	0
13.3	54.2	117.2	0	0	0	0
11.2	121.3	152.3	175.2	0	0	0
8	109.1	124.5	107.5	391.6	0	0
6.7	54.2	111	67.1	76	616	0
0	85	180.1	98.7	116.7	0	723

A.2.3: Product mass retained using a 12 mm gap size.

Sieve (mm)	A	B	C	D	E	F
	803 g	**679 g**	**740 g**	**700 g**	**673 g**	**768 g**
16	329	0	0	0	0	0
13.3	232.2	434.1	0	0	0	0
11.2	80	142.2	606.2	0	0	0
8	88	54	96	700	0	0
6.7	23.9	13.2	14.3	0	673	0
0	40	27	22	0	0	768

Appendix B: Breakage matrices

B.1: Breakage matrices constructed from the ratio of the retained product mass to the initial mass for Test 1:

B.1.1: 8 mm gap size breakage matrix for Test 1.

Sieve size (mm)	A	B	C	D	E	F
16	0.086	0.000	0.000	0.000	0.000	0.000
13.3	0.082	0.150	0.000	0.000	0.000	0.000
11.2	0.060	0.120	0.090	0.000	0.000	0.000
8	0.057	0.140	0.110	0.160	0.000	0.000
6.7	0.142	0.080	0.130	0.080	1.000	0.000
0	0.573	0.510	0.670	0.760	0.000	1.000

B.1.2: 10 mm gap size breakage matrix for Test 1.

Sieve size (mm)	A	B	C	D	E	F
16	0.250	0.000	0.000	0.000	0.000	0.000
13.3	0.130	0.210	0.000	0.000	0.000	0.000
11.2	0.230	0.190	0.430	0.000	0.000	0.000
8	0.200	0.180	0.190	0.700	0.000	0.000
6.7	0.110	0.170	0.220	0.200	1.000	0.000
0	0.160	0.220	0.160	0.100	0.000	1.000

B.1.3: 12 mm gap size breakage matrix for Test 1.

Sieve size (mm)	**A**	**B**	**C**	**D**	**E**	**F**
16	0.350	0.000	0.000	0.000	0.000	0.000
13.3	0.210	0.570	0.000	0.000	0.000	0.000
11.2	0.140	0.170	0.720	0.000	0.000	0.000
8	0.130	0.120	0.210	1.000	0.000	0.000
6.7	0.060	0.050	0.040	0.000	1.000	0.000
0	0.110	0.090	0.030	0.000	0.000	1.000

B.2. Breakage matrices constructed from the ratio of the retained product mass to the initial mass for Test 2:

B.2.1: 8 mm gap size breakage matrix for Test 2.

Sieve (mm)	**A**	**B**	**C**	**D**	**E**	**F**
16	0.100	0.000	0.000	0.000	0.000	0.000
13.3	0.100	0.200	0.000	0.000	0.000	0.000
11.2	0.070	0.030	0.050	0.000	0.000	0.000
8	0.130	0.070	0.090	0.240	0.000	0.000
6.7	0.100	0.100	0.060	0.060	1.000	0.000
0	0.500	0.600	0.800	0.700	0.000	1.000

B.2.2: 10 mm gap size breakage matrix for Test 2.

	A	**B**	**C**	**D**	**E**	**F**
16	0.300	0.000	0.000	0.000	0.000	0.000
13.3	0.090	0.170	0.000	0.000	0.000	0.000
11.2	0.200	0.220	0.390	0.000	0.000	0.000
8	0.180	0.180	0.240	0.670	0.000	0.000
6.7	0.090	0.160	0.150	0.130	1.000	0.000
0	0.140	0.260	0.220	0.200	0.000	1.000

B.2.3: 12 mm gap size breakage matrix for Test 2.

	A	**B**	**C**	**D**	**E**	**F**
16	0.410	0.000	0.000	0.000	0.000	0.000
13.3	0.290	0.640	0.000	0.000	0.000	0.000
11.2	0.100	0.210	0.820	0.000	0.000	0.000
8	0.110	0.080	0.130	1.000	0.000	0.000
6.7	0.030	0.020	0.020	0.000	1.000	0.000
0	0.050	0.040	0.030	0.000	0.000	1.000

Appendix C: Prediction of PSD using matrices

C.1: Prediction using an 8 mm gap size breakage matrix for Test 1.

Feed PSD (g)		8 mm breakage matrix (Test 1)							Sim P.PSD (g)	Exp P. PSD
58		0.086	0	0	0	0	0		**4.988**	**0**
62		0.082	0.15	0	0	0	0		**14.056**	**8**
161	x	0.06	0.12	0.09	0	0	0	=	**25.41**	**43.4**
230		0.057	0.14	0.11	0.16	0	0		**66.496**	**93.7**
63		0.142	0.08	0.13	0.08	1	0		**115.526**	**113**

C.2: Prediction using a 10 mm gap size breakage matrix for Test1.

Feed PSD (g)		10 mm breakage matrix (Test 1)							Sim P.PSD (g)	Exp P. PSD
26		0.25	0	0	0	0	0		**6.5**	**16.3**
30		0.13	0.21	0	0	0	0		**9.68**	**23.5**
86	x	0.23	0.19	0.43	0	0	0	=	**48.66**	**32.7**
103		0.2	0.18	0.19	0.7	0	0		**99.04**	**71.6**
31		0.11	0.17	0.22	0.2	1	0		**78.48**	**85.3**
308		0.16	0.22	0.16	0.1	0	1		**342.82**	**338.7**

C.3: Prediction using an 8 mm gap size breakage matrix for Test 2.

Feed PSD (g)		8 mm breakage matrix (test2)							Sim P.PSD (g)	Exp P. PSD
58		0.1	0	0	0	0	0		**5.8**	**0**
62		0.1	0.2	0	0	0	0		**18.2**	**8**
161	x	0.07	0.03	0.05	0	0	0	=	**13.97**	**43.4**
230		0.13	0.07	0.09	0.24	0	0		**81.57**	**93.7**
63		0.1	0.1	0.06	0.06	1	0		**98.46**	**113**
583		0.5	0.6	0.8	0.7	0	1		**939**	**898.6**

C.4: Prediction using a 10 mm gap size breakage matrix for Test 2.

Feed PSD (g)		10 mm breakage matrix (Test 2)							Sim P.PSD (g)	Exp P. PSD
26		0.3	0	0	0	0	0		**7.8**	**16.3**
30		0.09	0.17	0	0	0	0		**7.44**	**23.5**
86	x	0.2	0.22	0.39	0	0	0	=	**45.34**	**32.7**
103		0.18	0.18	0.24	0.67	0	0		**99.73**	**71.6**
31		0.09	0.16	0.15	0.13	1	0		**64.43**	**85.3**
308		0.14	0.26	0.22	0.2	0	1		**358.96**	**338.75**

Appendix D: Impact of feed size on PSD

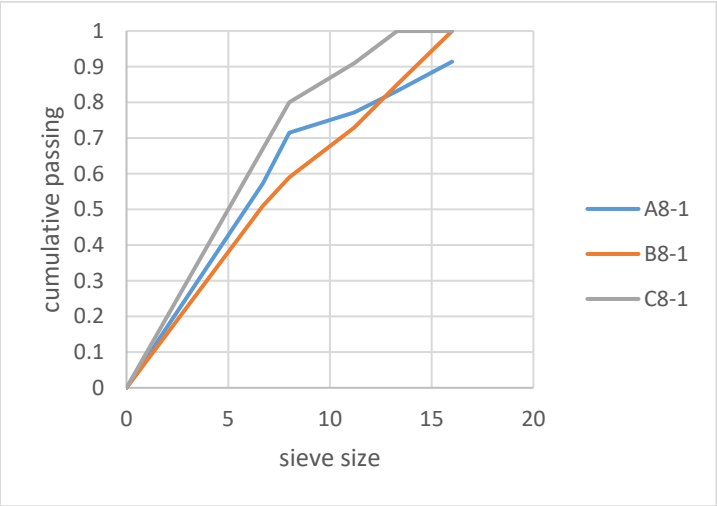

D.1: PSD from the milling of A, B, and C through an 8 mm gap size for Test 1.

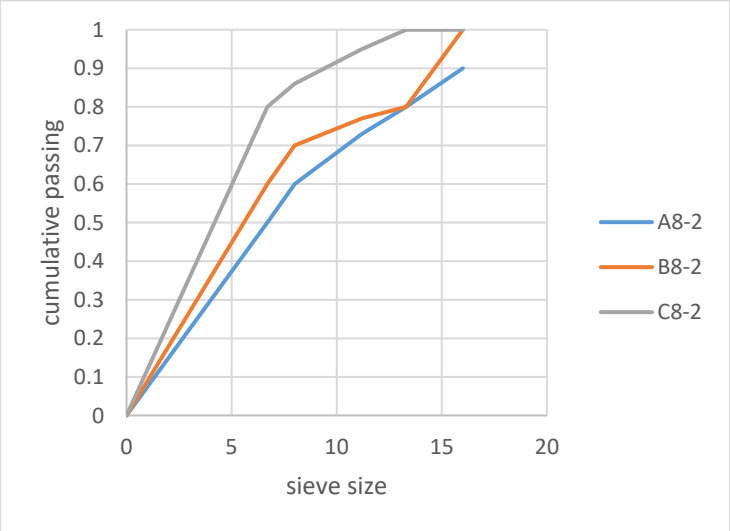

D.2: PSD from the milling of A, B, and C through an 8 mm gap size for Test 2.

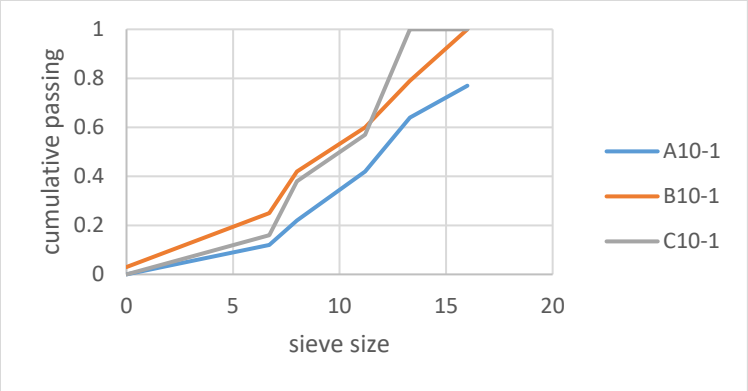

D.3: PSD from the milling of A, B, and C through a 10 mm gap size for Test 1.

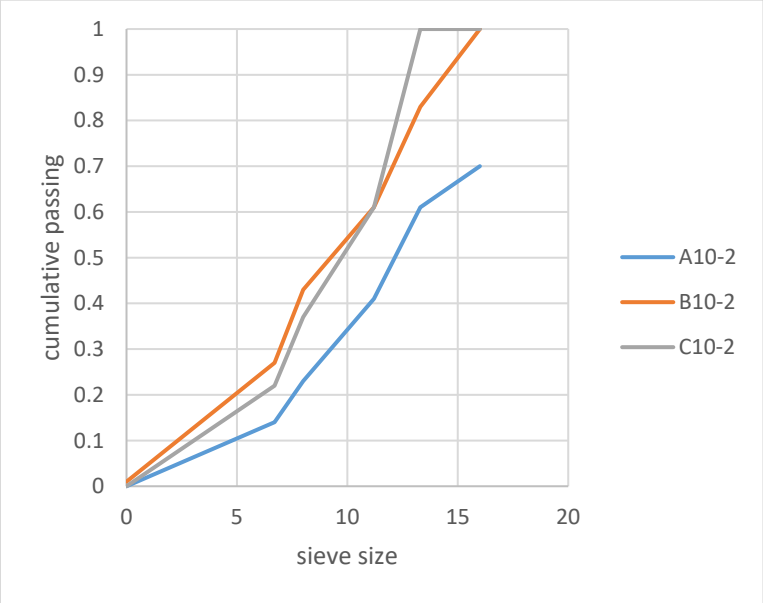

D.4: PSD from the milling of A, B, and C through a 10 mm gap size for Test 2.

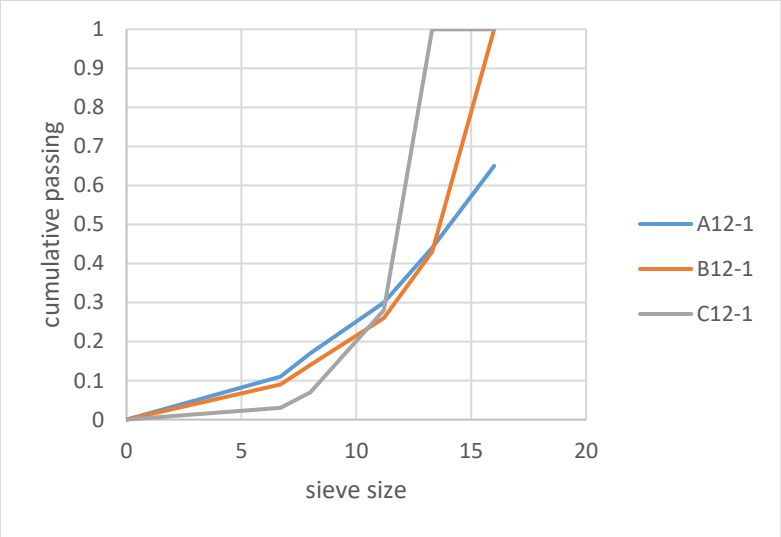

D.5: PSD from the milling of A, B, and C through a 12 mm gap size for Test 1.

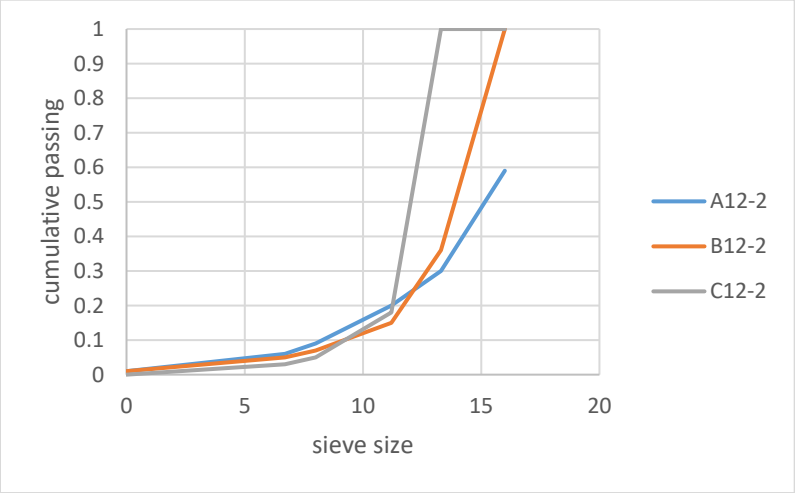

D.6: PSD from the milling of A, B, and C through a 12 mm gap size for Test 2.

Appendix E: Impact of feed mass on PSD

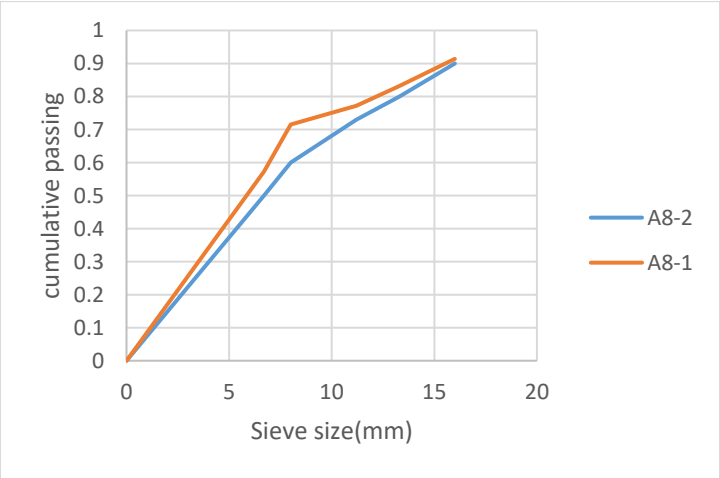

E.1: Comparison of PSD from the milling of size class A, using 701 g for Test 2 and 469 g for Test 1 through an 8mm gap size.

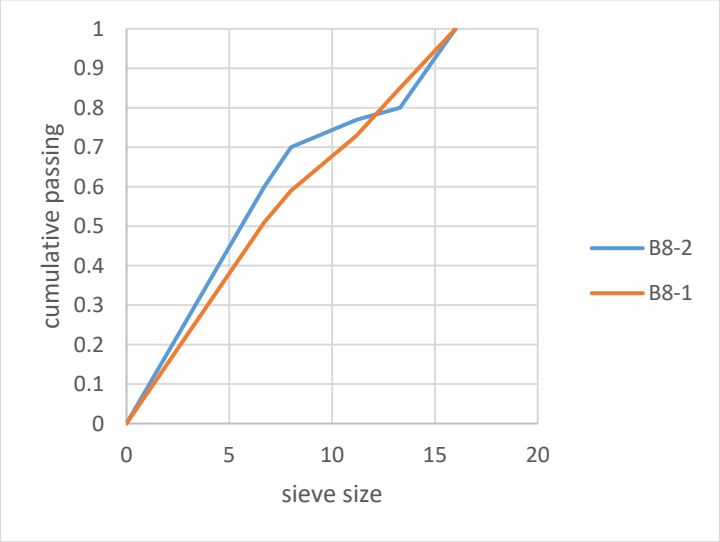

E.2: Comparison of PSD from the milling of size class B using 652 g for Test 2 and 457 g for Test 1 through an 8mm gap size.

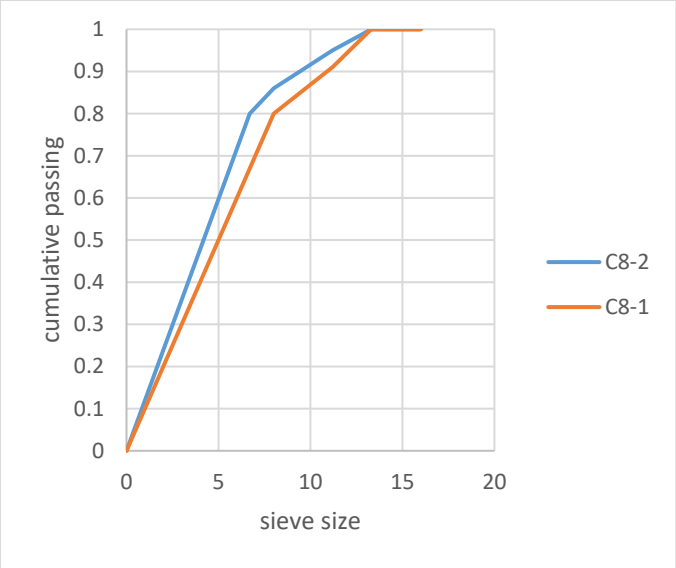

E.3: Comparison of PSD from the milling of size class C, using 731 g for Test 2 and 629 g for Test 1, through an 8mm gap size.

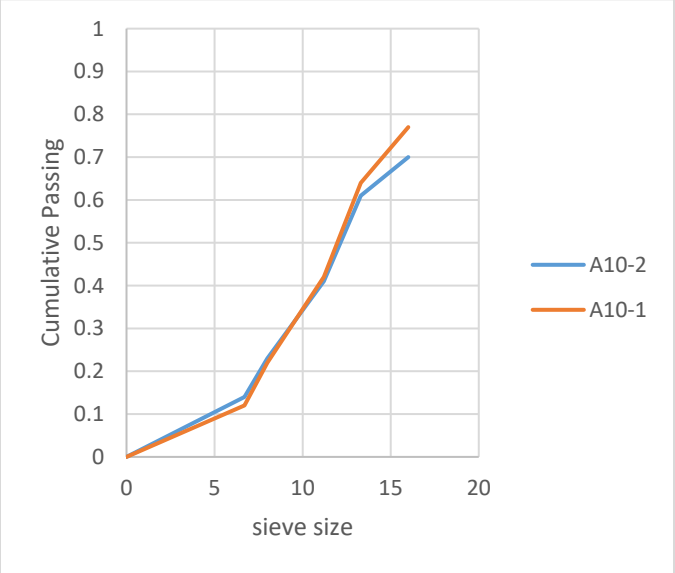

E.4: Comparison of PSD from the milling of size class A using 609 g for Test 2 and 906 g for Test 1 through a 10mm gap size.

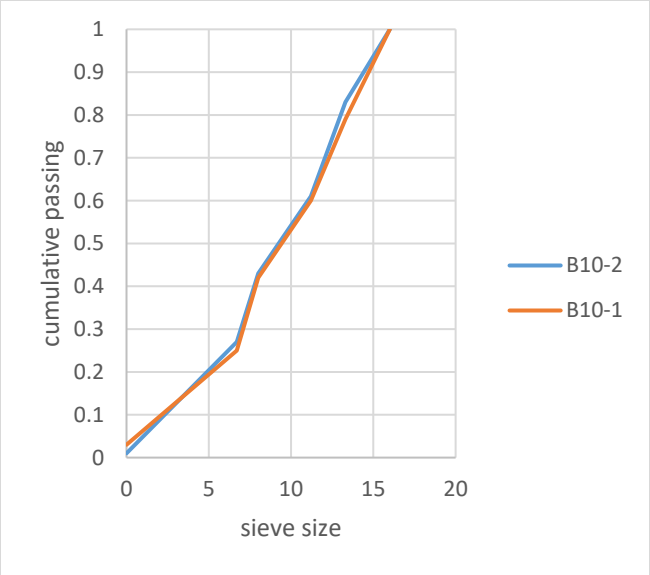

E.5: Comparison of PSD from the milling of size class B using 694 g for Test 2 and 635 g for Test 1 through a 10mm gap size.

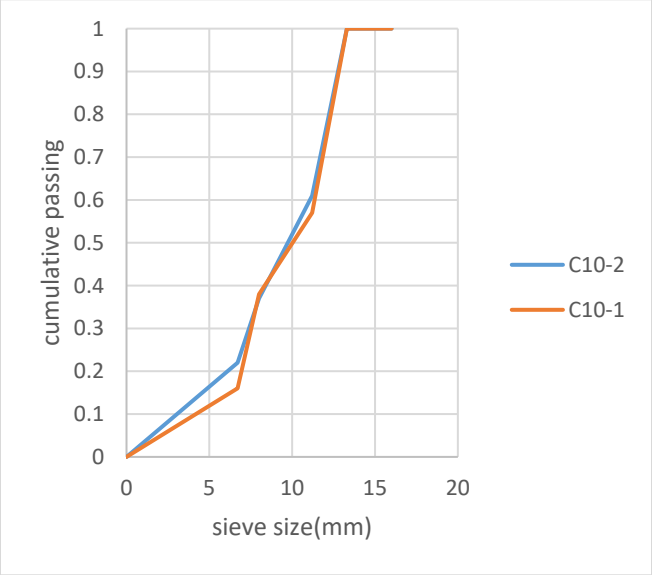

E.6: Comparison of PSD from the milling of size class C using 450 g for Test 2 and 407 g for Test 1 through a 10mm gap size.

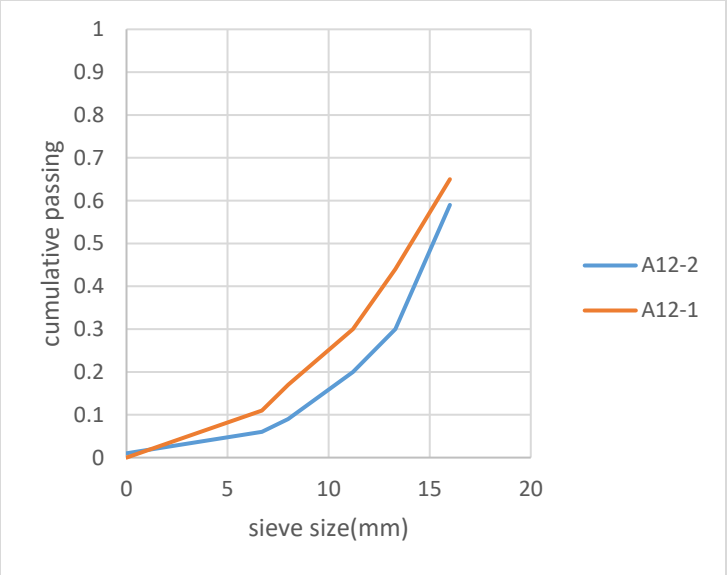

E.7: Comparison of PSD from the milling of size class A using 803 g for Test 2 and 860 g for Test 1 through a 12mm gap size.

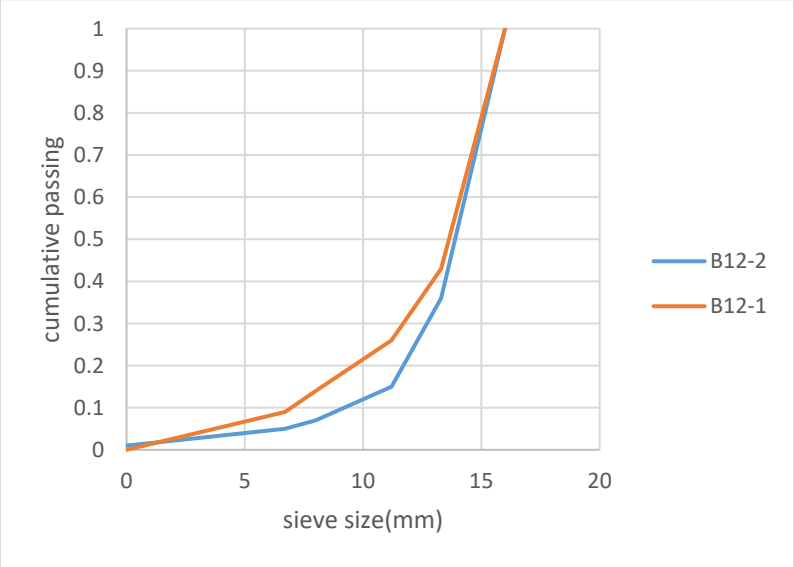

E.8: Comparison of PSD from the milling of size class B using 679 g for Test 2 and 769 g for Test 1 through a 12 mm gap size.

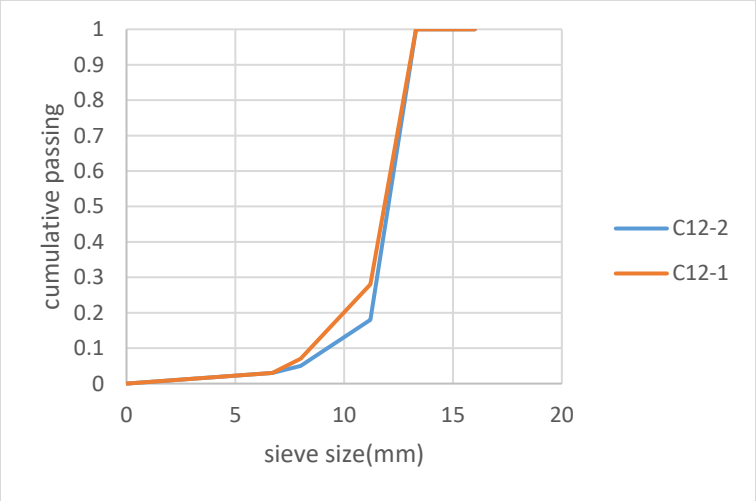

E.9: Comparison of PSD from the milling of size class C using 740 g for Test 2 and 728 g for Test 1 through a 12 mm gap size.

Appendix F: Milling ratio Vs Cumulative passing

F.1: Cumulative passing for a 8 mm gap size.

Sieve (mm)	8/17	8/14.65	8/12.25
17	0.9	1	1
14.65	0.8	0.8	1
12.25	0.73	0.77	0.95
9.6	0.6	0.7	0.86
7.35	0.5	0.6	0.8
3.35	0	0	0

F.2: Cumulative passing for a 10 mm gap size.

Sieve (mm)	10/17	10/14.65	10/12.25
17	0.7	1	1
14.65	0.61	0.83	1
12.25	0.41	0.61	0.61
9.6	0.23	0.43	0.37
7.35	0.14	0.27	0.22
3.35	0	0.01	0

F.3: Cumulative passing for a 12 mm gap size.

	12/17	**12/14.65**	**12/12.25**
17	0.59	1	1
14.65	0.3	0.36	1
12.25	0.2	0.15	0.18
9.6	0.09	0.07	0.05
7.35	0.06	0.05	0.03
3.35	0.01	0.01	0

Appendix G: Breakage function modeling

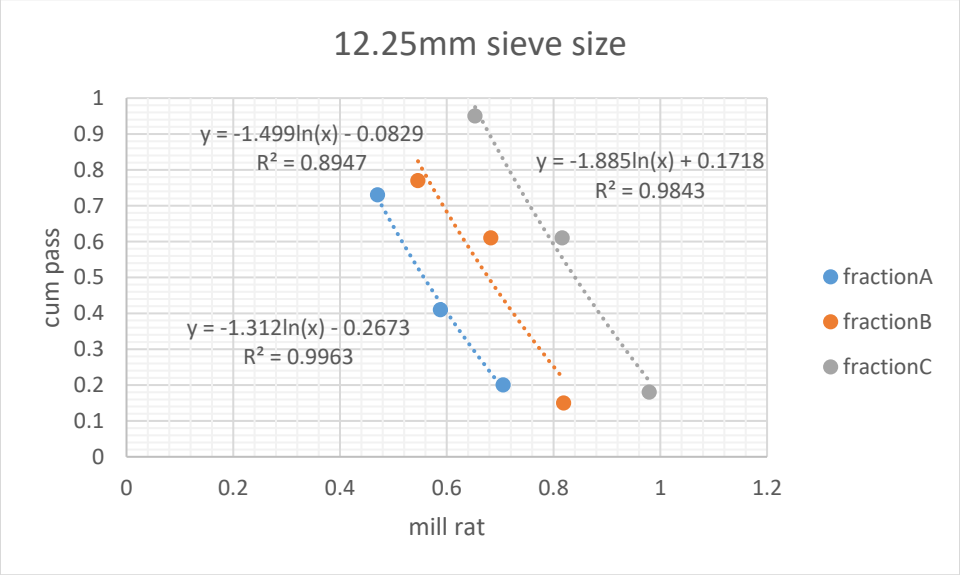

G.1: Cumulative passing with a 12.25 mm sieve size versus milling ratio.

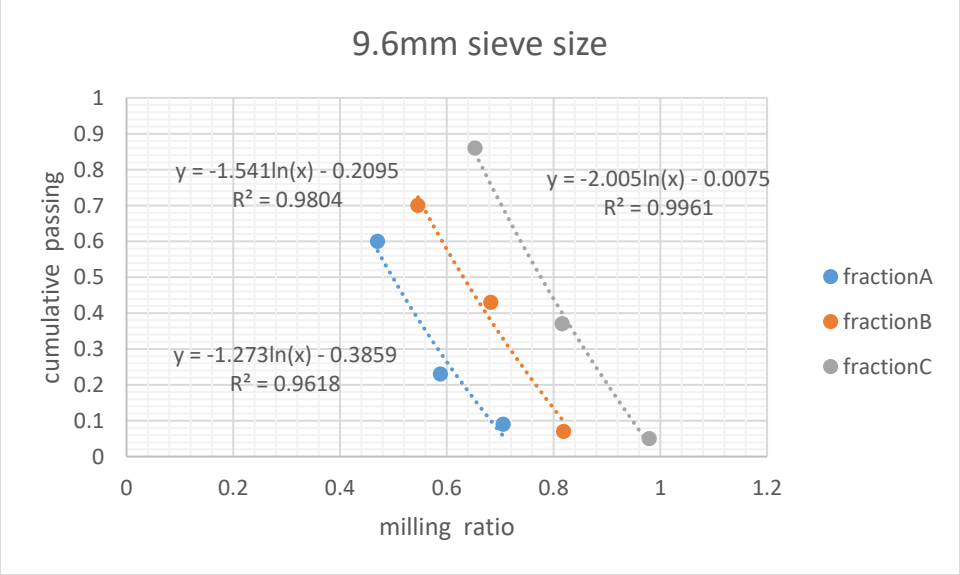

G.2: Cumulative passing with a 9.6 mm sieve size versus milling ratio.

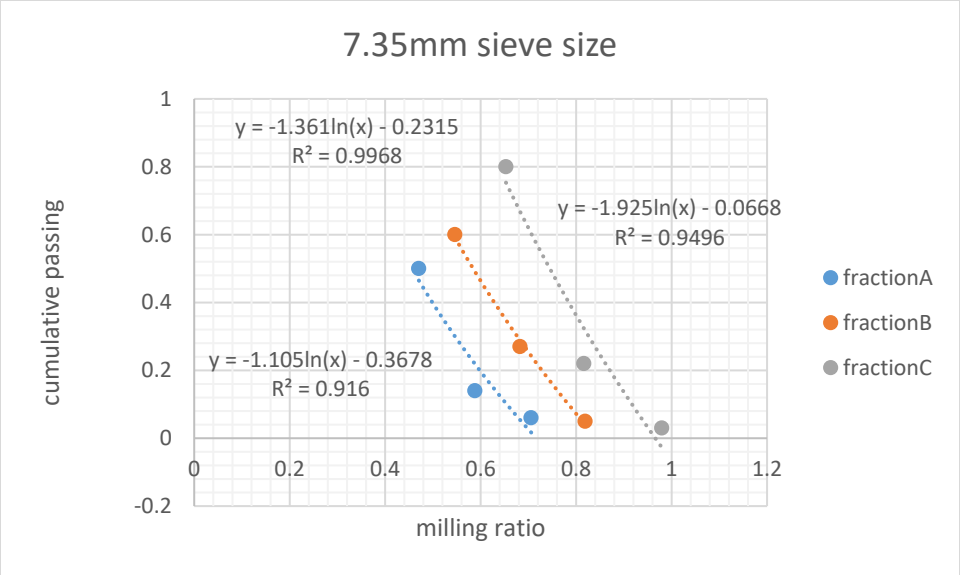

G.3: Cumulative passing with a 7.35 mm sieve size versus milling ratio.